

1 **Hydrochemical and isotopic evidences for deciphering conceptual model of groundwater**
2 **Delineating multiple salinization processes in a coastal plain aquifer, northern China: hydrochemical and isotopic evidence**

5 Han Dongmei^{a,b}, Matthew Currell^c

6 a Key Laboratory of Water Cycle & Related Land Surface Processes, Institute of Geographic Sciences and Natural Resources
7 Research, Chinese Academy of Sciences, Beijing, 100101, China

8 b College of Resources and Environment, University of Chinese Academy of Sciences, Beijing 100049, China

9 c School of Engineering, RMIT University, Melbourne VIC 3000, Australia.

10 **Abstract**

11 Groundwater is ~~the an~~ important water resource for agricultural irrigation, urban ~~and tourism development~~
12 and industrial utilization in the coastal regions of ~~northern~~ China. In the past five decades, coastal
13 groundwater salinization in the Yang-Dai River ~~coastal~~ plain has become ~~more increasingly~~ serious ~~than~~
14 ~~ever before~~ under ~~the influence of natural climate change and anthropogenic activities and climatic change~~.
15 It is pivotal for the scientific management of coastal water resources to accurately understand groundwater
16 salinization processes and ~~its induceement~~~~their causative factors~~. Hydrochemical ~~(major ion and trace~~
17 ~~element)~~ and stable isotopic ($\delta^{18}\text{O}$ and $\delta^2\text{H}$) analysis ~~for of the~~ different water bodies (surface water,
18 groundwater, geothermal water, and seawater) were ~~applied conducted~~ to ~~provide a better improve~~
19 understanding of ~~the processes of~~ groundwater salinization ~~processes~~ in ~~the the plain's~~ Quaternary aquifers.
20 Saltwater intrusion ~~due to intensive groundwater pumping~~ is ~~the a~~ major ~~aspect process, and can be caused~~
21 ~~by either by~~ vertical infiltration along ~~the~~ riverbeds ~~which convey saline surface water inland, at the~~
22 ~~downstream areas of rivers during the tide/surge period, and/or direct subsurface~~ lateral inflow ~~into fresh~~
23 ~~aquifer derived from intensively pumping groundwater. Trends in salinity with depth indicate that the~~
24 ~~former may be more important than previously assumed. The Seawater proportion of seawater in~~
25 ~~groundwater is estimated to have ean reached up to ~13% in the shallow groundwater of a local~~ well field.
26 ~~End-member mixing calculations also indicate that hHighly~~ mineralized geothermal water (TDS ~~of~~ up to
27 10.6 g/L) ~~with depleted stable isotope compositions and elevated strontium concentrations (>10 mg/L) with~~
28 ~~the indicator of paleoseawater relies (lower Cl/Br ratios relative to modern seawater) also locally overflows~~
29 ~~mixes with water into the cold overlying Quaternary aquifers. This is particularly evident in samples with~~
30 ~~elevated Sr/Cl ratios (>0.005 mass ratio). Groundwater Deterioration of groundwater quality by~~ salinization
31 ~~ean is also be also clearly~~ exacerbated by ~~the~~ anthropogenic ~~activities~~ pollution. Nitrate contamination via
32 ~~intrusion of heavily polluted marine water is evident locally (e.g. in the Zaoyuan well field); however, more~~

widespread nitrate contamination due to other local sources such as (e.g., irrigation return flow with solution of fertilizers and/or domestic wastewater) is evident on the basis of NO_3/Cl ratios discharge. Additionally, the interaction between surface water and groundwater can make the groundwater freshening or salinizing in different sections to locally modify the groundwater hydrochemistry. The cease of the well field and establishment of anti-tide dam in the Yang River estuary area have effective function to contain the development of saltwater intrusion. This study provides an example of how multiple geochemical indicators can delineate different salinization processes and guide the future water management practices, and provide research approaches and foundation for further investigation of seawater intrusion in this a densely populated water-stressed coastal region and similar region.

Key words: Groundwater salinization; Stable isotopes; Coastal aquifers; Water quality

1. Introduction

Coastal regions is are the key areas for the world's social and economic development. Approximately 40% of the world's population live within 100 kilometers of the coast (UN Atlas, 2010). The worldwide, coastal these areas have become increasingly urbanized, with 14 of the world's 17 largest cities located along coasts (Creel L, 2003). China has 18,000 km of continental coastline, about and around 164 million people (about approximately 12% of the total Chinese population) living in 14 coastal provinces, and nearly 80% of these people inhabit in the three coastal 'economic zones' economic regions, namely Beijing-Tianjin-Hebei economic region, the Yangtze River delta economic region and the Pearl River delta economic region (Shi, 2012). The rapid economic development and the growing population in these coastal regions have greatly increased demands for fresh water, meanwhile Meanwhile, been they are also confronted with the threat from increased waste and sewage and other waste water discharge into coastal ecosystems environments.

Coastal Groundwater resources play crucial roles on in the social, economic and ecologic function in of the global coastal systems (IPCC, 2007). Coastal groundwater Coastal aquifers system connect withs the ocean and with the continental hydro-ecological systems (Moore, 1996; Ferguson and Gleeson, 2012). Groundwater as an important freshwater resource, groundwater could may be over-extracted due to that the during periods of highest demand, which (e.g., agricultural irrigation and tourist seasons) are often the periods of lowest recharge and/or surface water availability rates (Post, 2005). In addition to occurrence of some environmental issues, such as land subsidence, contaminants transport, the overexploitation of

groundwater can therefore readily result in seawater intrusion in the coastal area, as well as related environmental issues such as land subsidence. Seawater intrusion has become a global issue and the related studies can be found from the coastal aquifers system of different countries around the world, such as including Israel (Sivan et al., 2005; Yechieli et al., 2009; Mazi et al., 2014), Spain (Price and Herman, 1991; Pulido-Leboeuf, 2004; Garing et al., 2013), France (Barbescot et al., 2000; de Montety et al., 2008), Italy (Giambastiani et al., 2007; Ghiglieri et al., 2012), Morocco (Bouchaou et al., 2008; El Yaouti et al., 2009), USA (Gingerich and Voss, 2002; Masterson, 2004; Langevin et al., 2010), Australia (Zhang et al., 2004; Narayan et al., 2007; Werner, 2010), China (Xue et al., 2000; Han et al., 2011, 2015), Vietnam (An et al., 2014), Indonesia (Rahmawati et al., 2013), India (Radhakrishna, 2001; Bobba, 2002) and Brazil (Montenegro et al., 2006; Cary et al., 2015), etc. Werner et al. (2013) gave an excellent provides a comprehensive review on of seawater intrusion processes, investigation and management.

A variety of approaches have been used to investigate seawater intrusion, including head measurement, geophysical methods, geochemical methods (environmental tracers combined hydrochemical and isotope data), conceptual and mathematical modeling (see reviews by Jones et al., 1999; Werner et al., 2013).

Seawater/saltwater intrusion is a complicated hydrogeological process, due to the impact of aquifer properties, anthropogenic activities (e.g., intensive groundwater pumping, irrigation practices), recharge rates, variable density flow, between the estuary and adjacent fresh groundwater system, tidal/surge activity and effects relating to global climate change, such as sea level rise (Ghassemi et al., 1993; Robinson et al., 1998; Smith and Turner, 2001; Simpson and Clement, 2004; Narayan et al., 2007; Werner and Simmons, 2009; Wang et al., 2015). Understanding the complex interactions between groundwater, surface water, and seawater is thus essential for effective management of coastal water resources (Mondal et al., 2010). Brockway et al. (2006) reported the negative relationship between saltwater intrusion length and river discharge. Understanding the complex interactions between groundwater and surface water, groundwater and seawater is essential for the effective management of water resources (Sophoeleus, 2002; Mondal et al., 2010). There was a vastly different salinization patterns may arise as a result of diverse interactions result based on numerical simulations in coastal settings for the additional distance of intrusion in the Nile Delta Aquifer of Egypt and in the Bay of Bengal under the same sea level rise (Sherif and Singh, 1999; Bobba, 2002; Westbrook et al., 2005). Bobba (2002) also employed numerical simulations to demonstrate an apparent risk of saltwater intrusion in the Godavari delta, India due to sea level rise. Westbrook et al. (2005) defined the hyporheic transition zone of mixing between river water and

93 groundwater influenced by tidal fluctuations and the contaminant distribution. Modelling
94 seawater intrusion in the Burdekin Delta irrigation area, North Queensland (Australia) has shown that
95 generally, seawater intrusion is far more sensitive to groundwater pumping and recharge rates and recharge
96 than to aquifer properties (e.g., hydraulic conductivity), and compared to the effects of groundwater
97 pumping, the effect in comparison to of tidal fluctuation and sea level rises on saltwater intrusion can be
98 neglected (Narayan et al., 2007; Ferguson and Gleeson, 2012). However, most models of seawater intrusion
99 require simplification of the coastal interface zone. Relatively rare few studies have focused on delineating
100 the complex interactions among the surface-ground-sea-water continuums in estuarine environmentss, and
101 including the effects of vertical infiltration of seawater into the off shore aquifers —through river channels,
102 vs. as compared to the sub-surface lateral landward migration of the freshwater-saltwater interface. Recent
103 data indicate that such processes may be more important in causing historical salinization of coastal
104 groundwater than previously appreciated (e.g. Cary et al., 2015; Lee et al., 2016; Larsen et al., 2017).

105 Additionally, groundwater in coastal aquifers may be affected by other salinization processes, such as
106 input of anthropogenic contaminants or induced mixing with saline water from deeper or adjacent
107 formations, which may include mineralized geothermal water or brines emplaced in the coastal zone over
108 geologic history.

109 The data of from China's marine environment bulletin released on March 2015 by the State Oceanic
110 Administration People's Republic of China showed that the major bays, including Bohai Bay, Liaodong
111 Bay and, Hangzhou Bay, are polluted seriously polluted, with the inorganic nitrogen and active phosphate
112 being tas the major pollutants (SOA, 2015). Seawater intrusion in China is the most serious around in the
113 Circum-Bohai-Sea region (Han et al., 2011; Han et al., 2016a); and due to the heavy marine pollution, If the
114 escalating impacts of anthropogenic activities on groundwater quality seawater intrusion in the future may
115 be not simply be a case of a simple problem related to groundwater salinization simple salt-water intrusion.
116 This region is also characterized by deep brines and geothermal waters (e.g. Han et al., 2014), which may
117 migrate and mix with fresher groundwater under due to intensive water extraction. Depending on the
118 specific processes involved, additional contaminants may mix with fresh groundwater resources in parallel
119 with seawater intrusion, and in this region, it is thus likely to be more difficult to mitigate and remediate
120 groundwater pollution caused by the contaminated seawater.

121 A variety of approaches can be used to investigate and differentiate seawater intrusion and other
122 salinization processes, including time-series water level and salinity measurements, geophysical methods,

conceptual and mathematical modeling as well as geochemical methods (see reviews by Jones et al., 1999; Werner et al., 2013). Geochemical techniques are particularly valuable in areas where the dynamics of saline intrusion are complicated and may involve long-term processes pre-dating accurate water level records, or where multiple salinization processes may be occurring simultaneously. These techniques typically employ the use of major ion ratios such as Cl/Br and Cl/Na, which are indicative of solute origins (Edmunds, 1996; Jones et al., 1999). Other ionic ratios, involving Mg, Ca, Na, HCO₃ and SO₄, and characterization of water 'types' can also be useful in determining the geochemical evolution of coastal groundwater, for example, indicating freshening or salinization, due to commonly associated ion exchange and redox reactions (Anderson et al., 2005; Walraevens, 2007). Trace elements such as strontium, lithium and boron can provide additional valuable information about sources of salinity and mixing between various end-members, as particular waters can have distinctive concentrations (and/or isotopic compositions) of these elements (e.g., Vengosh et al., 1999). Stable isotopes of water ($\delta^{18}\text{O}$ and $\delta^2\text{H}$) are also commonly used in such studies, as they are sensitive indicators of water and salinity sources, allowing seawater to be distinguished from other salt sources (e.g., Currell et al., 2015).—

This study ~~will takeexamines~~ the Yang-Dai River coastal plain in Qinhuangdao City, Hebei province ~~of~~ north China, ~~specifically focusing on salinization of fresh groundwater caused by groundwater exploitation in the Zaoyuan well field and surrounding areas.~~ ~~The study as an example to~~ investigates groundwater salinization processes and interactions among surface water, ~~groundwater and~~ seawater ~~and~~ geothermal groundwater, ~~and~~ in a dynamic environment, with significant pressure on water resources ~~the seawater intrusion caused by groundwater exploitation in Zaoyuan well field.~~ Qinhuangdao is an important port and tourist city of northern China. In the past 30 years, many ~~sprevious~~ studies ~~had done to have~~ investigated ~~d~~ distribution of seawater intrusion and its influencing factors ~~in the region~~ using hydrochemical analysis ~~of groundwater~~ (Xu, 1986; Yang *et al.*, 1994, 2008; Chen and Ma, 2002; Sun and Yang, 2007; Zhang, 2012) and numerical simulations (Han, 1990; Bao, 2005; Zuo, 2009). ~~However, these studies have yet to provide clear resolution of the different mechanisms contributing to salinization, and have typically ignored the role of anthropogenic pollution and groundwater-surface water interaction.~~ This study is ~~thus~~ a continuation of previous investigations of the ~~coastal plain aquifers in Qinhuangdaoregion~~, ~~using a range of~~ hydrochemical and stable isotopic ~~eompositions of collected water samples were analyzed for~~ data to ~~making up the knowledge gap of surface~~, ground and sea water interactions in this ~~region.~~ This study aims to describe the conceptual model of the complex processes for the groundwater

153 salinization of the coastal aquifers, to reveal delineate the major aspects processes responsible for the
154 increasing groundwater salinity in the coastal aquifers, including lateral sub-surface sea-water intrusion,
155 vertical leakage of marine-influenced surface water, induced mixing of saline geothermal water, and
156 anthropogenic pollution. The goal is to and to obtain a more robust conceptual model model for
157 deciphering of the interconnections between groundwater the various water sources under the impact of
158 groundwater exploitation flow system of the study area. The results will be helpful for the further
159 numerical simulations of coastal groundwater system. It is provide very significant new information for to
160 assist water resources management in the coastal plain of Bohai bay, and other similar coastal areas
161 globally.

162 2. Study area

163 The Yang-Dai River coastal plain (Fig. 1) covers approximately 200km² in of the west side of
164 Beidaihe District of Qinhuangdao City, the northeastern Hebei Province. It connects the eastern section of is
165 surrounded by the Yanshan Mountain Mountains to the north and west, and and surrounded by mountains.
166 The southern boundary of the study area is the Bohai Sea. The plain become low from declines in
167 topographic elevation (with an average slope of 0.008) from approximately 390m above sea-level in the
168 northwest to 1-25m in the southeast, forming and a fan-shaped distribution of the incised piedmont-coastal
169 inclined alluvial plain sediments. Elevation ranges from 390 in the west and to 40-100 m in the north, and
170 25-40 in the east, and 25-1m in the south coastal region, with the average slope of 0.008. Zaoyuan well
171 field, located in the southern edge of the alluvial fan, approximately 4.3km from the Yang River estuary,
172 was built in 1959 (Xu, 1986) as a major water supply for this the region. It is 4.3 km from the southeastern
173 well field to Yang River estuary (Fig. 1).

174 2.1 Climate and hydrology

175 The study area is in a warm and semi-humid monsoon climate. On the basis of a 56-a-year record in
176 Qinhuangdao area, the mean annual rainfall is estimated to be approximately 640 mm, the average annual
177 temperature is about approximately 11°C, and mean potential evaporation of 1469 mm. 75% of the total
178 annual rainfall falls in July-September (Zuo, 2006), during the East Asian Summer Monsoon. The average
179 annual tide level is 0.86m (meters above Yellow Sea base level), while the highest and low tides is are
180 approximately 2.48m, and the lowest is 1.43m.

181 The Yanghe River and Daihe River, originated from the Yanshan Mountains, are the major surface

water bodies in this area, flowing southward into the Bohai Sea (Fig. 1). The Yang River is approximately 100 km long with a catchment area of 1029 km^2 and average annual runoff of $1.11 \times 10^8 \text{ m}^3/\text{a}$ (Han, 1988). Dai River has a length of 35 km and catchment area of 290 km^2 , with annual runoff of $0.27 \times 10^8 \text{ m}^3/\text{a}$. The rivers become soared full during when heavy intense rain events happened with short peak duration, whereas it and revert to become minimal flow or drying during the dry season – in part this is related to impoundment of flow in upstream reservoirs. The Yang River is about 100 km long with the catchment area of 1029 km^2 , and the average annual runoff of $1.11 \times 10^8 \text{ m}^3/\text{a}$ (Han, 1988). Dai River has the length 35 km and catchment area of 290 km^2 , with annual runoff of $0.27 \times 10^8 \text{ m}^3/\text{a}$ and average gradient of 11.4‰. The two rivers flow into the southern Bohai Sea.

2.2 Geological and hydrogeological setting

Groundwater in this area mainly includes water in Quaternary porous sediment fissure as well as fractured bedrock water in the bedrock and water in the Quaternary porous media. The bedrock fissure water is distributed in the northern platform area. Its water abundance is Fractured rock groundwater volume mainly dependsed on the degree of weathering and the nature and regularity of fault zones (Fig. 1). The strata outcropping in the west, north and eastern edge of the plain includes the Archean gneiss, Proterozoic mixed granite and and Jurassic aged metamorphic and igneous rocks, which also underlie the The ex Quaternary, which is exposed in the offshore area of the region, is mainly the Archean metamorphic granite, which is widely distributed. The mineral composition includes mainly quartz, feldspar, and biotite. The Quaternary sediments of the plain (from which most samples in this study were collected) are mostly underlain by the Archean gneisses and Proterozoic mixed granites. The basement faults under the Quaternary cover are mainly include the NE-trending fault and the NW-trending (Fig. 1) fault. The Quaternary aquifer system of the Yang-Dai River coastal plain is a complete groundwater system from the piedmont to the coast (see P-P' cross-section of Figure 2). these Geological techniques structures control the development and deformation thickness of the overlying sediments, as well as the distribution of hot springs and geothermal anomalies. Fault zones are also thought to be the main channel for deep water cycle and transport of thermal convection water from deeper to shallower depths.

The Quaternary sediments are widely distributed in the area, with the thickness ranging from approximately 5-80 m (mostly 20-40 m), up to more than 100 m immediately adjacent to the coastline. The bottom of the Holocene (Q_4) unit in most areas has clay or consists of clay layers, which make making the

groundwater in the coastal zone ~~under-confined or semi-confined status, although~~. There are no regional, continuous aquitards between several layers of aquifer-forming sediments (Fig. 21bB) ~~aquifers. The thickness of the Quaternary strata has a range of 5-80 m, mostly 20-40 m, and up to more than 100 m near the coastline.~~ The aquifer is mainly composed of medium sand, coarse sand and gravel layers with ~~thickness of 10-20 m and~~ water table depth of 1-4 m in the phreatic aquifer, and deeper semi-confined groundwater (where present and hydraulically separated from the phreatic aquifer) ~~thickness of 10-30 m and hosted in similar deposits with a water table depth~~ potentiometric surface of 1-5 m below topographic elevation in the confined aquifer (Zuo, 2006).

~~In the yearly peak season of agricultural water, the groundwater level decline sharply and reaches the lowest water table in April-May period, and become highest in January-February. The main sources of aquifer recharge are from rainfall infiltration, river water and irrigation return-flow, lateral subsurface runoff from the piedmont area. Apart from the phreatic water evaporation, groundwater pumping is the main pathway of groundwater discharge for agricultural, industrial, tourism and sanatorium's utilization. The general flow direction of groundwater is from northwest to south, according to the topography. The main sources of recharge are from infiltration of rainfall, river water and irrigation return-flow, as well as lateral subsurface inflow from the piedmont area. Naturally, groundwater discharges into the rivers and the Bohai Sea. Apart from phreatic water evaporation, groundwater pumping for agricultural, industrial and domestic usage (including seasonal tourism) are currently the main pathways of groundwater discharge.~~

~~The geothermal water discharges into shallow Quaternary sediments near the fault zones, discharges into shallow Quaternary sediments, which is the overlying strata in evident as geothermal anomalies (Hui, 2009). The temperature of thermal water ranges is from 27-57°C in this low-to-medium temperature geothermal field (Zeng, 1991). The thickness of the overlying strata is varied from 24.6 to 58.8 m and consists of alluvial sand, gravel, clayey loam, clay and silt. The deeper thermal water is stored in the Archaeozoic granite and metamorphic rocks, which are composed of migmatite, gneiss, and amphibole plagiogneiss (Pan, 1990). Major deep fracture zones are the good provide pathways passage for the geothermal water movement (Yang, 2011). The heated groundwater in the deep zones could upward transport along the fault and mix with into the overlying cold groundwater in the Quaternary aquifers sediments (Pan, 1990; Shen et al., 1993; Yang, 2011).~~

239 **2.3 Environmental issues****Groundwater usage** and seawater intrusion history

240 The shallow groundwater pumped from the Quaternary aquifer occupies 94% of the total
241 groundwater exploitation, and is which is used for agricultural irrigation (accounts for 52% of the total
242 groundwater use), industrial (32%) and domestic water (16%) (Meng, 2004). Many large and
243 medium-sized reservoirs were built in the 1960s and 1970s and resulted in meaning that the surface water
244 was intercepted and the downstream runoff dropped sharply, even became causing rivers to dry up in
245 drought years. With the intensification of human socio-economic activities and growing urbanization,
246 coupled with extended drought years (severe drought during 1976-1989 in north China) (Wilhite, 1993; Han
247 et al., 2015), increased groundwater exploitation to meet the ever-growing fresh water demands has
248 resulted in groundwater level declining and seawater intrusion (SWI) in the coastal aquifers.

249 The pumping rate in the Zaoyuan well field was gradually increased from 1.25 million m³/a in the
250 early 1960s to 3.5 million m³/a in the late 1970s, and beyond 10 million m³/a in the 1980s. During
251 1966-1989, the major agricultural planting in this region isof paddy fields became common, with
252 big resulting in significant agricultural water consumption. This caused formation of a cone of depression in
253 the Quaternary aquifer system. The groundwater pumping time is in this region mainly occurs from May
254 to October in spring and early summer, with typical pumping rates of 7~80,000 m³/d. Pumping from
255 the Zaoyuan well-field occurs in wells approximately 15 to 20m deep, which was over exploited and
256 resulted in formation of groundwater level declining depression. Groundwater levels decline sharply and
257 reach their lowest level during May, before the summer rains begin, and recover to their yearly high in
258 January-February (Fig. 2). In May 1986, the groundwater level in the depression center, which is located in
259 Zaoyuan-Jiangying (Supplementary Figure S1), was decreased to below 2 m.a.s.l. (meters above sea
260 level), with the depression area, which has with groundwater levels below the sea level, covered 28.2
261 km². The local government commenced reduction in groundwater exploitation in this area after 1992, and
262 groundwater levels began to decrease more slowly after 1995, even showing recovery in some wells.
263 However, during an extreme drought year (1999), increased water demand resulted in renewed
264 groundwater level declines in the region (Fig. 32). Since 2000, the groundwater levels have responded
265 seasonally to water demand peaks and recharge (Fig. 2; Fig. S1).

266 Since From 1990, the rapid development of township enterprises in the 1980s (mainly refer to paper
267 mills), also began to cause groundwater over-exploitation in the western area of the plain. The
268 groundwater i.e. the groundwater pumping rate for paper mills development reached 55,000 m³/d in 2002.

269 resulting in the groundwater level depressions around Liushouying and Fangezhuang (Fig. 1). The lowest
270 groundwater level in the western depression center associated with this pumping in 1991 was up to reached
271 -11.6 m.a.s.l. in 1991, and -17.4 m.a.s.l. in 2002. After the implementation of “Transferring Qing River
272 water to Qinhuangdao” project since in 1992, the intensity of groundwater pumping generally became
273 slowed down reduced, and the depression center moved to Liushouying area. The groundwater level of
274 the in the depression center was recovered to -4.3 m.a.s.l. in July 2006.

275 Overall, the depression area (groundwater levels below mean sea level) was recorded as 132.3km² in
276 May 2004 and the shape of the depression was has generally been elliptical with the major axis of
277 the aligned E-W direction. The depression area developed to 132.3km² in May 2004. In addition to
278 groundwater over-exploitation, climate change-induced recharge reduction has also likely contributed to
279 groundwater level declines and hence seawater intrusion (Fig. S2). The annual average rainfall declined
280 from 639.7 mm between 1954 - 1979 to 594.2 mm between 1980-2010; a significant decrease over the last
281 30 years (Zhang, 2012). As indicated in Figure S2, the severity of seawater intrusion (indicated by changes
282 in Cl concentration, and the total area impacted by SWI, as defined by the 250mg/L Cl contour) correlates
283 with periods of below average rainfall – indicated by monthly cumulative rainfall departure (CRD, Weber
284 and Stewart, 2004).

285

286 The groundwater quality of this area has become gradually became more salineized since from the
287 early 1980s, with chloride concentrations increasing year by year. As early as 1979, seawater intrusion
288 occurred was recorded in the Zaoyuan well field. The intrusion area with groundwater chloride
289 concentration greater than 250 mg/L has been developed was to 21.8 km² in 1984, and 32.4 km² in 1991,
290 52.6 km² in 2004 and, 57.3 km² in 2007 (Zuo, 2006; Zang et al., 2010). The chloride concentration of
291 groundwater pumped from the a monitored well-field well (depth of 18 m, this well field G10 in Fig. 1)
292 changed from 90 mg/L in 1963 to 218 mg/L in 1978, 567 mg/L in 1986, 459 mg/L in 1995, and 1367 mg/L
293 in 2002 (Zuo, 2006), reducing to 812 mg/L in July 2007 (this study). The distance of estimated seawater
294 intrusion into the inland area from the coastline had reached 6.5 km inland in 1991, and developed to 8.75
295 km in 2008 (Zang et al., 2010). At In the early 1990s, 16 of 21 pumping wells in the well field have
296 been were abundant abandoned due to the salineized water quality (Liang et al., 2010). Additionally, 370 of
297 520 pumping wells were abandoned has been abundant in the wider Yang-Dai River coastal plain during
298 1982-1991 (Zuo, 2006).

300

3. Methods

301 ~~Totally~~ In total, 80 water samples were collected from the Yang-Dai River coastal plain, including 58
 302 groundwater samples, 19 river water samples (from 12 sites), and 3 seawater samples, during three
 303 sampling campaigns, namely, (June 2008, September 2009 and August 2010). Groundwater samples were
 304 pumped from 28 productive wells with well depths of between 6 and 110m, including 7 deep
 305 wells with, which has well depths greater than 60m (Fig. 1). While ideally, sampling for geochemical
 306 parameters would be conducted on monitoring wells, due to an absence of these, production wells were
 307 utilised. In most cases, the screened interval of these wells encompasses aquifer thicknesses of
 308 approximately 5 to 15m above the depths indicated in Table 1.

309 ~~The water sampling sites can be shown in Figure 1.~~ In this study, we sampling investigated focused
 310 predominantly on low temperature cold groundwater, from the productive wells. However, the
 311 geothermal water existing from around Danihe cannot be ignored was also considered a potentially
 312 important ongoing source of groundwater salinity. As such, while geothermal water samples were not
 313 accessible during our sampling campaigns (as the area is now protected). The related data can be available
 314 and referenced data reported by Zeng (1991) due to that we cannot obtain the hot water samples from
 315 the current geothermal field were compiled and analyzed in conjunction with the sampled wells.

316 Measurements of some physico-chemical parameters (i.e. pH, temperature, and electrical
 317 conductivity (EC)) were conducted in situ using a portable meter (WTW Multi 3500i). All water samples
 318 were filtered to 0.45- μ m membrane filters before collection for analysis of hydrochemical composition.
 319 Two aliquots in polyethylene 100mL bottles at each site were collected for major cation and anion analysis,
 320 respectively. Samples for cation analysis (Na^+ , K^+ , Mg^{2+} and Ca^{2+}) were added treated with 6-N HNO_3 to
 321 prevent precipitation. Water samples were sealed and stored at 4°C until determination analysis.
 322 Bicarbonates was determined by titration within 12 hours after sampling. The concentrations
 323 of cations and some trace elements (i.e. B, and Sr, Li) were analyzed by inductively coupled plasma-optical
 324 emission spectrometry (ICP-OES) on filtered samples in the chemical laboratory of the Institute of
 325 Geographic Sciences and Natural Resources Research (IGSNRR), Chinese Academy Sciences (CAS). Only
 326 the Sr data are reported here, as the other trace elements were not relevant to the interpretations discussed
 327 (Table 1). The detection limits for analysis of Na^+ , K^+ , Mg^{2+} and Ca^{2+} are 0.03, 0.05, 0.009, and 0.02 mg/L.

Concentrations of major anions (i.e. Cl^- , SO_4^{2-} , NO_3^- and F^-) were analyzed ~~by using~~ a High Performance Ion Chromatograph (SHIMADZU, LC-10ADvp) at the IGSNRR, CAS. ~~The detection limits for analysis of Cl^- , SO_4^{2-} , NO_3^- and F^- are 0.007, 0.018, 0.016, and 0.006 mg/L. The testing precision the cation and anion analysis is 0.1-5.0%. The ion Charge balance errors of the chemical results were are less than 8%. The hydrochemical and physical data are shown in Table 1. The stable isotopes ($\delta^{18}\text{O}$ and $\delta^2\text{H}$) of water samples were measured ~~by using~~ a Finnigan MAT 253 mass spectrometer after on-line pyrolysis with a Thermo Finnigan TC/EA in the Stable Isotopes Laboratory of the IGSNRR, CAS. The results are expressed in % relative to international standards (V-SMOW (Vienna Standard Mean Ocean Water)) and of resulting $\delta^{18}\text{O}$ and $\delta^2\text{H}$ values are shown in Table 1. were expressed in % relative to international standards (V-SMOW (Vienna Standard Mean Ocean Water)). The analytical precision for $\delta^2\text{H}$ is $\pm 2\%$ and for $\delta^{18}\text{O}$ is $\pm 0.5\%$. All hydrochemical, physico-chemical and isotope data are reported in Table 1.~~

~~Saturation indices for common minerals (i.e. calcite, dolomite, and gypsum) were calculated using PHREEQC version 2.8 (Parkhurst and Appelo, 1999) to understand the saturation status of these minerals in the aquifer. Ionic delta values were calculated to further investigate the hydrogeochemical behavior that take place in the aquifer and modify groundwater hydrochemistry. The ionic delta values express enrichment or depletion of each ion's concentration relative to its theoretical concentration. Mixing calculations were also conducted on the basis of calculated from the Cl^- concentrations of the samples under for a conservative freshwater-seawater mixing system (Fidelibus et al., 1993; Appelo, 1994). The delta values have been used as effective indicators of coastal groundwater undergoing freshening or salinizing processes, accompanied by related water rock interaction (prevailingly cation exchange). Cl^- can be regarded as a conservative tracer for the calculations mentioned below. The seawater contribution for each sample can be expressed by as a fraction of seawater (f_{sw}), which can be calculated using (Appelo and Postma, 2005):~~

$$f_{sw} = \frac{C_{Cl,sam} - C_{Cl,f}}{C_{Cl,sw} - C_{Cl,f}} \quad (1)$$

~~where $C_{Cl,sam}$, $C_{Cl,f}$, and $C_{Cl,sw}$ refer to the Cl^- concentration in the sample, freshwater, and seawater, respectively. Based on the f_{sw} value, the theoretical concentration ($C_{i,mix}$) of each ion in a water sample can be calculated by:~~

$$C_{i,mix} = f_{sw} \cdot C_{i,sw} + (1 - f_{sw}) \cdot C_{i,f} \quad (2)$$

356 $C_{i,sw}$ and $C_{i,f}$ refer to the measured concentration of the ion i in the seawater and freshwater,
357 respectively. The ionic delta value (ΔC_i) of ion i can be obtained by:

358
$$\Delta C_i = C_{i,sam} - C_{i,mix} \quad (3)$$

359 $C_{i,sam}$ the measured concentration of the ion i in the water sample.

361 4. Results

362 4.1 Groundwater dynamics

363 Due to the different groundwater pumping rate and patterns, the variation trend of groundwater level
364 has been different in the east and west areas of the Yang-Dai River coastal plain. In the east part, owing to
365 the intensive exploitation in the Zaoyuan well field, the groundwater level was gradually declined to be
366 lower than the sea level during the 1980s. The center of groundwater level depression was located in
367 Zaoyuan Jiangying region, with the groundwater level lower than 3 m.a.s.l. The local government
368 commenced to reduce the exploitation after 1992. The groundwater level decreased slowly after 1995, even
369 started to recovery in some wells as a result of pumping reduction. During the extreme drought year (1999),
370 the consequential increased water demand made the groundwater level declined again in the east region. In
371 the late 1980s, the groundwater level at the west region was still more than 0 m.a.s.l. But in the late 1990s,
372 due to the fast development of the local paper mills as the big water consumers, the groundwater level
373 dropped year by year and had big falling amplitude after 2000, resulting in the overall transfer of
374 groundwater depression center to the western region (Liushouying Fangzhuang). The groundwater level in
375 this center was up to 14 m.a.s.l. in May 2002.

376 Based on the data from the three monitoring wells, the seasonal variation of groundwater level in this
377 area can be seen from Figure 3. After 2000, the groundwater level in the east of the Yang-Dai River coastal
378 plain was mainly affected by the groundwater pumping for agricultural and domestic water use. During
379 March and June of each year, the shallow groundwater pumping as the major water source for irrigation has
380 resulted in the fast dropped water level occurred between April and June, down to the lowest level of water
381 throughout the year. As the rainy season started in July, groundwater pumping began to decrease.
382 Groundwater level rise rapidly with the infiltration of irrigation return flow and rainfall, lateral subsurface
383 runoff from the surrounding aquifers. After the end of the rainy season (July to September), the water level
384 continues to rise gently and reach the annual maximum water level during January and February. With the

amount of recharge is reduced along with the increase of domestic water pumping, water level circularly slow down to the next agricultural peak. In addition to groundwater over exploitation, climate change induced recharge reduction in recent three decades has been also part of the cause of groundwater level declining, resulting in the seawater intrusion. The annual average rainfall varied from 639.7 mm (1954–1979) to 594.2 mm (1980–2010). It obviously finds that there is a significant decrease in rainfall over the last 30 years (Zhang, 2012). In general, the groundwater runoff intensity gradually decreases from the piedmont to the coastal region.

4.2.1 Water stable isotopes ($\delta^2\text{H}$ and $\delta^{18}\text{O}$)

The local meteoric water line (LMWL, $\delta^2\text{H}=6.6 \delta^{18}\text{O}+0.3$, $n=64$, $r^2=0.88$) is based on $\delta^2\text{H}$ and $\delta^{18}\text{O}$ mean monthly rainfall values between 1985 and 2003 from Tianjin station some 120 km SW of Qinhuangdao City (IAEA/WMO, 2006). Due to similar climate and position relative to the coast, this can be regarded as representative of the study area. 19 wSurface water samples collected from Yang River and Dai River ($n = 19$) have $\delta^{18}\text{O}$ and $\delta^2\text{H}$ values ranging from -10.1 to -0.6‰ (mean= -5.4‰) and from -71 to -11‰ (mean = -43‰), respectively. It seems that the stable isotopes compositions for surface water appear to exhibit have significant seasonal variation (Fig. S3). For Yang River, 3 surface water samples fromd in the relatively dry season (June 2008, $n = 3$) were characterized by had mean $\delta^{18}\text{O}$ and $\delta^2\text{H}$ values ranging from -5.5 to -1.1‰ (mean= of -3.0‰) and from -49 to -15‰ (mean = -31‰), respectively. Whereas 6 water samples sampleds in from the wet season (August 2009 and September 2010, $n = 6$) had meanve $\delta^{18}\text{O}$ and $\delta^2\text{H}$ values ranging from -10.1 to -2.4‰ (mean= of -6.6‰) and from -71 to -21‰ (mean = -48‰), respectively. As to Dai River, samples showed similar results; the dry season mean in dry season, 3 surface water samples are characterized by $\delta^{18}\text{O}$ and $\delta^2\text{H}$ values ($n = 3$) ranging from -3.9 to -0.6‰ (mean= were -2.6‰) and from -44 to -11‰ (mean = -32‰), respectively; and in wet season samples ($n = 7$), 7 surface water samples have had mean $\delta^{18}\text{O}$ and $\delta^2\text{H}$ values ranging from -9.7 to -1.2‰ (mean= of -6.6‰) and from -69 to -12‰ (mean = -49‰), respectively (Fig. 43).

The water samples collected from Yang River and Dai River have similar stable isotopes composition.

The 56 groundwater samples are were characterized by $\delta^{18}\text{O}$ and $\delta^2\text{H}$ values ranging from -11.0 to -4.2‰ (mean= -6.5‰) and from -76 to -39‰ (mean = -50‰), respectively. Among themthese, shallow and deep groundwater samples showed similar mean values, although deep groundwater samples ($n = 13$) showed relatively narrow overall ranges (43 shallow groundwater samples have $\delta^{18}\text{O}$ and $\delta^2\text{H}$ values

414 ranging from -11.0 to -4.2‰ (mean = -6.6‰) and from -76 to -39‰ (mean = -50‰), respectively; 13 deep
415 groundwaters have $\delta^{18}\text{O}$ and $\delta^2\text{H}$ values ranging from -7.8 to -5.1‰ (mean = -6.3‰) for $\delta^{18}\text{O}$; and
416 from -58 to -43‰ (mean = -50‰ for $\delta^2\text{H}$; Fig. 43), respectively. Slight seasonal variation was
417 evident in the groundwater isotope compositions; For the shallow groundwater from during the dry season
418 (n = 12) water samples have showed $\delta^{18}\text{O}$ and $\delta^2\text{H}$ values ranging from -7.2 to -4.2‰ (mean = -5.7‰) and
419 $\delta^2\text{H}$ values from -56 to -39‰ (mean = -48‰), respectively; while during the wet season (n = 31)
420 water samples are featured by $\delta^{18}\text{O}$ and $\delta^2\text{H}$ values ranged with a range of from -11.0 ~ -5.3‰ (mean =
421 -6.9‰) and -76 ~ -43‰ (mean = -51‰), respectively. Some variability was also evident in deep
422 groundwater compositions, although only three deep samples were collected during the dry season. For the
423 deep groundwater, during the dry season, 3 water samples have $\delta^{18}\text{O}$ and $\delta^2\text{H}$ values ranging from -5.3 to
424 -5.1‰ (mean = 5.2‰) and from -47 to -45‰ (mean = 46‰), respectively; during the wet season, 10 water
425 samples are featured by $\delta^{18}\text{O}$ and $\delta^2\text{H}$ values with a range of -7.8 ~ -5.2‰ (mean = -6.6‰) and -58 ~ -43‰
426 (mean = 51‰), respectively.

427 The local meteoric water line (LMWL, $\delta^2\text{H} = 6.6 - \delta^{18}\text{O} + 0.3$, n = 64, $r^2 = 0.88$) is based on $\delta^2\text{H}$ and $\delta^{18}\text{O}$
428 mean values of the monthly rainfall between 1985 and 2003 at Tianjin station some 120 km SW of
429 Qinhuangdao City. The data were obtained from International Atomic Energy Agency/World
430 Meteorological Organization (IAEA/WMO, 2006). Due to the similar climatic and coastal conditions
431 between Tianjin and Qinhuangdao, this meteoric water line can be regarded as the local meteoric water line
432 (LMWL) in this study. From Figure 43, it can be seen that surface water have exhibits a much more wider
433 range of $\delta^{18}\text{O}$ and $\delta^2\text{H}$ values relative to groundwater, with shallow groundwater in turn more spatially
434 variable than deep groundwater. Water samples collected in the wet season have showed more wider ranges
435 of $\delta^{18}\text{O}$ and $\delta^2\text{H}$ values relative to water sampled in the dry season. Most of water samples samples of all
436 types plot to the right of (below) the LMWL, with some surface water samples showing similar
437 compositions to the local seawater (Fig. 43). The local seawater plots below (more negative) than
438 typically assumed values (e.g. VSMOW = 0‰) for both $\delta^2\text{H}$ and $\delta^{18}\text{O}$, and this water appears to represents
439 an end-member involved in mixing with meteoric-derived waters in both ground and surface water (Fig.
440 43) enriched in isotopes and plots far below the LMWL.

441 4.3.2 Water salinity and major dissolved ions

442 TDS (total dissolved solids) concentrations of the surface water samples from Dai River have a range

443 from of 0.3g/L~31.4g/L with 22-78% Na^+ and, Ca^{2+} comprising 22-78% and 4-56.4% Ca^{2+} of total cations
444 and 36-91% Cl^- comprising 36-91% of total anions. The composition changes from, $\text{Ca}\cdot\text{Na}\cdot\text{Mg}\cdot\text{Cl}\cdot\text{HCO}_3$
445 to Na-Cl water type from the upstream to the downstream locations along with increasing salinity; Cl^-
446 concentrations vary from approximately 70 mg/L upstream to 16700 mg/L near the coastline, due to marine
447 influence. The Cl^- concentrations varied from about 70 mg/L in the upstream to 16700 mg/L near the
448 coastline. Similar variation occurs along the Yang River, the collected water samples have TDS
449 concentrations of between 0.3-26.1 g/L with increasing percentages concentrations and proportions
450 (33-91%) of Cl^- concentrations (63.2-14953.5 mg/L) from the up-reach stream to the down-reach stream
451 locations, with water types changed from $\text{Ca}\cdot\text{Na}\cdot\text{HCO}_3\cdot\text{Cl}\cdot\text{SO}_4$, $\text{Ca}\cdot\text{Mg}\cdot\text{Cl}\cdot\text{SO}_4\cdot\text{HCO}_3$, to Na-Cl. The
452 Nitrate contents concentrations also range from 2.8 to 65.2 mg/L in the surface water samples, increasing
453 downstream.

454 Groundwater hydrochemistry can be modified the comprehensive effects from geological, climatic,
455 hydrogeological processes and anthropogenic activities. In the early 1960s, groundwater pumped from the
456 Zaoyuan well field was featured by the exhibited Ca-HCO₃ water type and chloride concentrations of
457 90-130 mg/L; this was followed by rapid salinization since the 1980s (see section 2.3). In the early 1970s,
458 individual wells appear slightly salinized. It has been deteriorated rapidly since the early 1980s. The
459 chloride concentration of groundwater from water supply wells was 90mg/L in 1963, 218 mg/L in 1975,
460 385 mg/L in 1984, 456.3 mg/L in 1986, 459.5 mg/L in 1995, 928.3 mg/L in 2000, 1367 mg/L in 2002, and
461 1290.4 mg/L in 2005 (Zang et al., 2010). In this study, the shallow groundwater is characterized by TDS
462 concentrations of 0.4-4.8 g/L with the percentage of Cl^- (34-77%), Na^+ (12-85%) and, Ca^{2+} (5-69%) being
463 the predominant major anion and cations, respectively, and water Groundwater hydrochemical types varied
464 vary from Ca-HCO₃•Cl, Ca•Na-Cl, Na•Ca-Cl to Na-Cl, which can been seen from Piper plot (Figure 54).
465 The deep groundwater is featured by has TDS concentrations of between 0.3-2.8g/L, which is dominated
466 by Ca (up to 77% of major cations) in the upstream area and Na (up to 85% of major cations) near the coast,
467 with water type distributed in series of evolving from Ca-Cl•HCO₃ to, Ca•Na-Cl and Na•Mg-Cl (Figure 54).
468 At present, the TDS of groundwater from the well field reaches 3.31 g/L with Na-Cl water type in the (see
469 well G15). The relative high fracture The highest observed- mixing proportions of seawater occurs in the
470 shallow well G10 and deep well G2, respectively, with calculated f_{sw} values (according to equation 1) of
471 12.95% and 5.35%, respectively.

472 Hydrochemical features of thermal water from the Danihe-Luwangzhuang area (Fig. 1A) are distinct

473 from the normal/low temperature groundwater. Previous work by Zeng (1991) and Hui (2009) identified
474 geothermal water with high TDS in the fractures of deep metamorphic rock. The geothermal water was
475 characterized by TDS values between 6.2-10.6 g/L and Ca-Na-Cl water type, while Cl⁻ concentrations
476 ranged from 5.4 to 6.5 g/L and Sr concentrations from 6.73 to 89.8 mg/L. Some normal/low temperature
477 groundwater samples collected in this study from wells G8, G19, and G9 featured by Ca-Na-Cl water type
478 with relative high TDS ranges (0.8-1.4 g/L, 1.3-1.6 g/L, and 1.5-2.8 g/L, respectively) and strontium
479 concentrations (1.1-1.9 mg/L, 4.9-7.1 mg/L, and 7.3-11.6 mg/L, respectively), showing similarity with the
480 geothermal system. Low temperature groundwater sampled in this study had Sr/Cl mass ratios ranging from
481 2.4×10^{-4} to 1.6×10^{-2} , with higher ratios in deep groundwater (range: 9.4×10^{-4} to 1.3×10^{-2} ,
482 median: 3.7×10^{-3}) compared to shallow groundwater (median: 3.1×10^{-3}), and groundwater generally
483 higher than seawater/saline surface water (range: 3.7×10^{-4} to 5.8×10^{-4} , median: 3.9×10^{-4} ; Table S1).

484 The nitrate/Nitrate contents concentrations in groundwater have a range of from 2.0-178.5 mg/L (mean
485 90.1 mg/L) for shallow groundwater, and 2.0-952.1 mg/L (mean 232.1 mg/L) for the deep groundwater,
486 respectively, with most of which samples seriously exceeding the WHO drinking water standard (50
487 mg/L).

488 There is a geothermal field around Danihe-Luwangzhuang area (Fig. 1). Hydrochemical features of
489 thermal water are very distinct from cold water. The previous investigation has identified the buried
490 geothermal water with high TDS in the fracture/fissure of deep metamorphic rock (Zeng, 1991). Due to the
491 pumping wells for pumping thermal water were protected and not permitted to be sampled, we have to
492 collect some data associated this geothermal field from the previous research. The geothermal field is
493 controlled by the fault distribution under confined state. The thermal water flows along the fault zone and
494 enters the Quaternary aquifer, forming hot salt water distributed around the spill point and expanded
495 towards downstream. It can result in the similar hydrochemical characteristics between Quaternary salt
496 groundwater and deep original thermal waters from bedrocks. The geothermal water is characterized by
497 Ca-Na-Cl water type, 6.2-10.6 g/L of TDS and 7.4-8.7 of pH values. Cl⁻ concentrations range from 5.4 to
498 6.5 g/L, Na⁺ from 1.7 to 2.0 g/L, Ca²⁺ from 1.6 to 1.9 g/L, F⁻ from 3.0 to 3.6 mg/L, Sr from 6.73 to 89.8
499 mg/L, Li from 0.43 to 1.58 mg/L, and SiO₂ from 44.0 to 48.3 mg/L (Hui, 2009). The groundwater samples,
500 collected from the wells G8, G19, and G9 with different depths, are featured by Ca-Na-Cl water type with
501 relative high TDS ranges (0.8-1.4 g/L, 1.3-1.6 g/L, and 1.5-2.8 g/L, respectively) and Sr contents (1.1-1.9
502 mg/L, 4.9-7.1 mg/L, and 7.3-11.6 mg/L, respectively).

503 **5. Discussions**

504 **5.1 Groundwater flow systemisotopes and hydrochemical featureshydrochemistry as**
505 **indicators of mixing processes**

506 ~~Generally, The~~ Quaternary groundwater system in the Yang-Dai River coastal plain ~~is~~~~may~~ be
507 recharged by precipitation, irrigation return flow, river infiltration and lateral subsurface runoff ~~(e.g.~~ from
508 mountain-front regions~~s~~). ~~Due to the natural geological function and human pumping activities, there have~~
509 ~~been interactions between groundwater and geothermal waters around Danihe area or between groundwater~~
510 ~~and seawater in the coastal area. The g~~roundwater geochemical ~~features~~characteristics are ~~then~~ controlled
511 by ~~the complex~~ hydrogeological conditions and ~~these hydrological~~mixing processes, ~~including~~ mixing
512 ~~induced by extensive groundwater pumping, as well as natural mixing and water-rock interaction. It is~~
513 ~~evident from the geochemistry that mixing has occurred between groundwater and seawater in the coastal~~
514 ~~areas, as well as between normal/low temperature groundwater and geothermal water in the inland areas~~
515 ~~(e.g. near the Danihe geothermal field). The d~~ifferent sources of water ~~bodies~~ are ~~generally~~ characterized
516 by ~~somewhat distinctivedifferent of~~ stable isotopic and hydrochemical compositions, ~~allowing~~ mixing
517 ~~calculations to aid understanding of determining~~ the groundwater salinization ~~and mixing~~ processes, ~~as~~
518 ~~discussed below in this area.~~

519 ~~The s~~table isotopes of O and H ~~in groundwater and surface water~~ ~~can be used to describe the~~
520 ~~groundwater origin and to identify the mixing processes between different water bodies. The fall on a~~
521 ~~best-fit regression line slope of the best fit regression line for collected groundwater samples~~ (dashed line
522 in Fig. 43) ~~given as with slope of~~ $\delta^2\text{H} = 4.4 \times \delta^{18}\text{O} - 21.7$, ~~which is~~ significantly lower than either the local or
523 global meteoric water lines. ~~Three processes are likely responsible for the observed range of isotopic~~
524 ~~compositions: 1. Mixing between saline surface water (e.g. seawater or saline river water affected by tidal~~
525 ~~ingress) and fresher, meteoric-derived groundwater or surface water; 2. Mixing between fresh~~
526 ~~meteoric-derived groundwater and saline thermal water; 3. Evaporative enrichment of surface water and/or~~
527 ~~irrigation return-flow, which may The deviation of groundwater and surface water lines from the LMWL~~
528 ~~has evidenced evaporative processes occurred during water infiltrationion groundwater in some areas and~~
529 ~~surface runoff. A sub-group of surface water samples (e.g., S1 to S3, S7 and S12; termed 'brackish surface~~
530 ~~water') show marine-like stable isotopic compositions and major ion compositions (Fig. 43 and Fig. 5). The~~
531 ~~'fresh' surface water samples (e.g. EC values <1500 $\mu\text{S}/\text{cm}$) exhibit meteoric-like stable isotope~~
532 ~~compositions, with some samples (such as S9 and S10) showing clear evidence of evaporative enrichment~~

533 in the form of higher $\delta^2\text{H}$ and particularly, $\delta^{18}\text{O}$ values (Fig. 43).

534 Fresh groundwater has depleted $\delta^{18}\text{O}$ and $\delta^2\text{H}$ values relative to seawater and show a clear meteoric
535 origin, albeit with modification due to mixing. Theoretically, the mixing of meteoric-derived fresh
536 groundwater and marine water should result in a straight mixing line connecting the two end members;
537 however this is also complicated in the study area by the possible mixing with geothermal water. The
538 thermal groundwater has distinctive stable isotopic and major ion composition (Han, 1988; Zeng, 1991),
539 allowing these mixing processes to be partly delineated. Stable isotopes of thermal groundwater are more
540 depleted than low-temperature groundwater (e.g. $\delta^{18}\text{O}$ values of approximately -8‰, Fig. 8), indicating this
541 likely originates in the mountainous areas to the north; Zeng (1991) estimated the elevation of the recharge
542 area for the geothermal field to be from 1200 to 1500 m.a.s.l. Based on a bivariate plot of $\delta^{18}\text{O}$ vs. Cl^- with
543 mixing lines and defined fresh and saline end-members, Fig. 65 shows the estimated degree of mixing
544 between fresh groundwater including shallow (G4) and deep (G25) groundwater end-members, and saline
545 water, including seawater and geothermal end-members.

546 The two fresh end-members were selected to represent a range of different groundwater
547 compositions/recharge sources, from shallow water that is impacted by infiltration of partially evaporated
548 recharge (fresh but with enriched $\delta^{18}\text{O}$) to deeper groundwater unaffected by such enrichment (fresh and
549 with relatively depleted $\delta^{18}\text{O}$). The narrower range and relatively enriched stable isotopes in shallow
550 groundwater samples collected during the dry season compared with the wet season indicate some
551 influence of seasonal recharge by either rainfall (fresh, with relatively depleted stable isotopes) or irrigation
552 water subject to evaporative enrichment (more saline, with enriched stable isotopes and high nitrate
553 concentrations; Currell et al., 2010) and/or surface water leakage. While there is overlap in the isotopic and
554 hydrochemical compositions of shallow and deep groundwater (Fig. 3 & Fig. 4), this effect appears to only
555 affect the shallow aquifer.³⁴

556 Based on Fig. 5, the shallow groundwater samples (e.g. G15, G10, G11, G14) collected from or
557 around the Zaoyuan well field appear to be characterized by mixing between fresh meteoric water and
558 seawater (plotting in the upper part of Fig. 65); while some deeper groundwater samples (e.g. G13, G2,
559 G16, G14) collected from the coastal zone also appearing to indicate mixing with seawater. Groundwater
560 sampled relatively close to the geothermal field (e.g. G9, G19) shows compositions consistent with mixing
561 between low-temperature fresh water and saline thermal water (lower part of Fig. 5). This is more evident
562 in deep groundwater than shallow groundwater, which is consistent with mixing from below, as expected

563 for the deep-source geothermal water. Other samples impacted by salinization show more ambiguous
564 compositions between the various mixing lines, which may arise due to mixing with either seawater,
565 geothermal water or a combination of both (e.g., G29).

566 The estimated mixing fraction (f_{sw}) of marine water for the shallow brackish groundwater ranges from
567 1.2~13.0% and 2.6~6.0% for the deep brackish groundwater. The highest fraction of 13% was recorded in
568 G10, located in the northern part of the Zaoyuan well field, which is located near a tidally-impacted
569 tributary of the Yang River (Fig. 1). Relatively higher fractions of marine water in relatively shallow
570 samples (including those from the well field) compared to deeper samples may indicate a more ‘top down’
571 salinization process, related to leakage of saline surface water through the riverbed, rather than ‘classic’
572 lateral sea water intrusion, which typically causes salinization at deeper levels due to migration of a salt
573 water ‘wedge’ (e.g. Werner et al., 2013); this is consistent with results of resistivity surveys conducted in
574 the region (Fig. 6). –The profile of chloride concentrations vs. depth indicates that salinization affects
575 shallow and deep samples alike, with the most saline samples being relatively shallow wells in the
576 Zaoyuan well-field (Fig. 77). The composition of stable isotopes in groundwater samples collected in the
577 relatively dry season has been narrower and enricher than that collected in the wet season. It could be
578 resulted from evaporation processes during the infiltration of local irrigation return flows in the dry season.

579 The composition of stable isotopes for thermal groundwater could be originated from precipitation,
580 however, its ^{14}C age dating between 3.4~12.8ka with tritium content of less than 2 TU (Zeng, 1991),
581 indicating thermal waters might be formed under cooler climate condition than present climate. The
582 composition of stable isotopes of thermal groundwater are more depleted than that of cold groundwater,
583 even lower than the cold groundwater from mountain front area, indicating the thermal groundwater could
584 be mainly originated from NW mountain area, where has higher elevation. The elevation range of recharge
585 area for Danhe geothermal field is from 1200 to 1500 m.a.s.l obtained by Zeng (1991).

586 In general, brackish and fresh groundwater samples show distinctive major ion compositions, with the
587 more saline water typically showing higher proportions of Na and Cl (Fig. 54). This contrasts with historic
588 data collected from the Zaoyuan well field, which showed $\text{Ca}-\text{HCO}_3$ type water with Cl concentrations
589 ranging from 130 to 170 mg/L. This provides additional evidence that the salinization in this area is largely
590 due to marine water mixing. More Ca-dominated compositions are evident in the region near the
591 geothermal well field further in-land (e.g., G5, G8, G19, G29, and G24); consistent with a component of
592 salinization that is unrelated to marine water intrusion. Plots of ionic ratios of Na/Cl and Mg/Ca vs. Cl also

593 reveal a sub-set of relatively saline deep groundwater samples which appear to evolve towards the
594 geothermal-type signatures with increasing salinity (Fig. 88).

595 Stronger evidence of mixing of the geothermal water in the Quaternary aquifers (particularly deep
596 groundwater) is provided by examining strontium concentrations in conjunction with chloride (Fig. 99).
597 The geothermal water from Danihe geothermal field has much higher Sr concentrations (up to 89.8 mg/L)
598 than seawater (5.4-6.5 mg/L in this study), due to Sr-bearing minerals (i.e., celestite, strontianite) with Sr
599 contents of 300-2000 mg/kg present in the bedrock (Hebei Geology Survey, 1987). Groundwater sampled
600 from near the geothermal field in this study has the highest Sr concentrations e.g., G9 with Sr
601 concentrations ranging from 7.4 to 11.6 mg/L, and G19 from 4.9 to 7.1 mg/L.

602 The plot of chloride versus strontium concentrations (Fig. 99) shows that these samples and others
603 (e.g., G16, G20, G27, G29) plot close to a mixing line between fresh low-temperature and saline
604 thermal-groundwater. Mass ratios of Sr/Cl in these samples are also elevated relative to seawater by an
605 order of magnitude or more (e.g. $\text{Sr}/\text{Cl} > 5.0 \times 10^{-3}$, compared to 3.9×10^{-4} in seawater, Table S1). Other
606 samples from closer to the coast (e.g. G4) also approach the thermal-low temperature mixing line,
607 indicating probable input of thermal water. Samples collected from the Zaoyuan well field generally plot
608 closer to the Sr/Cl seawater mixing line (consistent with salinization largely due to marine water – Fig. 89);
609 however, samples mostly plot slightly above the mixing line with additional Sr, which may indicate more
610 widespread (but volumetrically minor) mixing with the thermal water in addition to seawater.

611 5.2 Anthropogenic pollution of groundwater

612 The occurrence of high nitrate (and possibly also sulfate) concentrations in groundwater in both
613 coastal and in-land areas also indicates that anthropogenic pollution is an important process impacting
614 groundwater quality and salinity (Fig. 1010; Table 1). Fresh groundwater has depleted $\delta^{18}\text{O}$ and $\delta^2\text{H}$ values
615 relative to seawater. Theoretically, the mixing of fresh groundwater and seawater should show a straight
616 line connecting the two end members. Obviously, some surface water samples (e.g. S1, S2, S3, S7, S12) are
617 the mixture with seawater. In this study area, there are three end members (namely, fresh groundwater,
618 thermal groundwater and seawater), which has been evidenced by the previous studies (Han, 1988; Zeng,
619 1991). Thus, the diagram of $\delta^{18}\text{O}$ vs. Cl^- (Fig. 6) can be used to identify the mixing pattern among three end
620 members. Fig. 6 shows the mixing lines between shallow fresh groundwater (G4) and seawater, between
621 deep fresh groundwater (G25) and seawater, between shallow fresh groundwater and thermal water, and

622 between deep fresh groundwater and thermal water. The shallow groundwater samples (e.g. G15, G10, G11,
623 G14) collected from or around the Zaoyuan well field are characterized by mixing with seawater. The deep
624 groundwater samples (e.g. G13, G2, G16, G14') collected from the coastal zone are also resulted from
625 mixing with seawater. The sampling site of deep groundwater sample G29 is located between thermal field
626 and the coastline and obviously affected by both of mixing processes. The groundwaters (e.g. G9, G19),
627 sampled from the area affected by geothermal field are mixture between fresh cold groundwater with
628 thermal waters. The mixing fraction (f_{sw}) of seawater has a range of 1.2–13.0% for the shallow brackish
629 groundwater, and 2.6–6.0% for the deep brackish groundwater. f_{sw} reaches the highest percentage of 13% in
630 the well G10, which is located in the north part of the well field.

631 At the late 1950s, groundwater pumped from the Zaoyuan well field was characterized by Ca-HCO₃
632 type water with Cl concentrations ranging from 130 to 170 mg/L. The hydrochemical data investigated in
633 1986 (Han, 1986) showed that there were mainly five water types in this study area, including Ca-HCO₃
634 type with TDS less than 0.5g/L distributed in the mountain front area, Ca-Na-Cl-SO₄, Ca-Na-Mg-SO₄-Cl,
635 or Na-Ca-Cl-SO₄ type water with TDS 0.4–0.7g/L distributed around the Zaoyuan well field and
636 Wanggezhuang, Ca-Na-Cl type water with TDS 0.4–1.8g/L distributed around the geothermal field
637 (Luwangzhuang) and Duzhai, Na-HCO₃ or Na-HCO₃-Cl type water with TDS 0.5–0.9g/L distributed the
638 SW area close to the coastal zone, and Cl-Na type water with TDS 0.4–2.4g/L distributed in the coastal
639 zone. Due to the disturbance of human activities, the current groundwater hydrochemistry has become more
640 complex than that before. Compared salty water distributed 2 km away from coastline in the late 1950s, the
641 distance has increased to about 7 km away from coastline. The Cl-Ca-Na or Cl-Ca type water type mainly
642 distributed in the area affected by geothermal field, such as G5, G8, G19, G29, and G24, indicating the
643 salinizing process during the mixing between cold groundwater and the thermal waters. In the upstream
644 area, the groundwater samples (e.g. G7, G23, G25) have feature of Ca-Mg-Na-Cl-SO₄, Ca-Cl-SO₄, and
645 Ca-Cl-HCO₃ type, not the Ca-HCO₃ type in the 1980s. It suggests that the salinized composition has
646 resulted from the anthropogenic pollution. The groundwater samples (e.g. G10, G11, G15, G26) collected
647 from the well field show the feature of Cl-Na-(Ca) type water with TDS 1.2–4.8 g/L. The samples (e.g. G1,
648 G2, G3, G4, G12, G22, G14, G14') collected from the coastal zone show the water type of Na-Cl or
649 Na-Ca-Cl-SO₄ or Ca-Na-Mg-Cl-SO₄, indicating that, apart from seawater intrusion, the anthropogenic
650 pollution also plays important role on modifying the groundwater chemistry.

651 The seawater from Bohai Sea has is heavily affected by nutrient contamination, showing relatively

652 higher- NO_3^- concentrations of 810 mg/L in this study, and up to 1092 mg/L in the coastal seawater further
653 north of the bay near of Dalian (Han et al., 2015), primarily due to wastewater discharge into the sea.
654 The historic sampled NO_3^- concentration of groundwater in the well field increased from 5.4 mg/L in May
655 1985 to 146.8~339.4 mg/L in Aug 2010, while the concentration of seawater in this area changed from
656 57.4 mg/L in May 1985 to 810.1 mg/L in Aug 2010. The diagram A bivariate plot (Fig. 7) of Cl^- vs. NO_3^-
657 concentrations of in groundwater (Fig. 10) can thus be used to identify nitrate sources and the different
658 mixing trends in this study area, including the mixing process with infiltration with contaminated seawater,
659 and and other on-land the anthropogenic NO_3^- -sources (e.g. domestic/industrial wastewater discharge and/or,
660 NO_3^- -bearing fertilizer input through precipitation infiltration and the irrigation return-flow) in the inland
661 area.

662 It can be seen from Fig. 7 this plot (Fig. 10) it appears that that the major source of NO_3^- in
663 groundwater is from on-land anthropogenic inputs rather than mixing with seawater, which would result in
664 relatively large increases in Cl^- along with NO_3^- , with the exception of Samples G10 and G15 (from the well
665 field) are exceptions to this trend, showing clear mixing with nitrate-contaminated seawater in the
666 well field. The deep groundwater (e.g. G9, G14) is also extensively contaminated by with higher NO_3^-
667 concentrations, this which is likely associated with leakage from the surface via the poorly constructed or
668 abandoned wells - a problem of growing significance in China (see Han et al., 2016b; Currell and Han,
669 2017). According to one investigation by Zang et al.(2010), 14 of 21 pumping wells in the Zaoyuan well
670 field have been abandoned due to the salinized poor water quality, and 307 pumping irrigation wells
671 (occupied 2/3 of total pumping wells for irrigation) in the region have also been abandoned. However, the
672 local department authorities have however not made any implemented measures to deal with those
673 abandoned wells, meaning they are a future legacy contamination risk – e.g. by allowing surface runoff
674 impacted by nitrate contamination to infiltrate down well annuli.

675 5.2.3 Groundwater salinization processes Hydrochemical evolution during salinization –

676 A hydrogeochemical facies evolution diagram (HFE-D) proposed by Giménez-Forcada (2010), was
677 used to analyze the geochemical evolution of groundwater during seawater intrusion and/or freshening
678 phases (Fig. 14). In the coastal zone, the river water shows an obvious mixing trend between fresh and
679 saline end members. Some shallow groundwaters (e.g., G2, G4, G10, G13, G15) are also close to the
680 mixing line between the surface-water end-members on this figure, indicating mixing with seawater

681 without significant additional modification by typical water-rock interaction processes (e.g. ion exchange).
682 Most brackish groundwaters (e.g., G11, G16, G17, G20, G25, G28, G29) have evolved in the series
683 $\text{Ca}-\text{HCO}_3 \rightarrow \text{Ca}-\text{Cl} \rightarrow \text{Na}-\text{Cl}$, according to classic seawater intrusion. A relative depletion in Na (shown in
684 lower than marine Na/Cl ratios) and enrichment in Ca (shown as enriched Ca/SO_4 ratios) is evident in
685 groundwater with intermediate salinities (e.g. Fig. 88; Fig. 101), indicating classic base-exchange between
686 Na and Ca during salinization (Appelo and Postma, 2005). Locally, certain brackish water samples (e.g.,
687 G1, G12, G26) appear to plot in the 'freshening' part of the HFE diagram (potentially indicating slowing or
688 reversal of salinisation due to reduced in groundwater use), although these do not follow a conclusive
689 trajectory. Water samples from the geothermal field (G5, G8, G9, and G19) plot in a particular corner of the
690 HFE diagram away from other samples (being particularly Ca-rich); a result of their distinctive
691 geochemical evolution during deep transport through the basement rocks at high temperatures.—

692 **5.2.1 Development of seawater intrusion and associated hydrochemical behavior**

693 The intensively pumping groundwater from the Quaternary aquifer of Yangtze River coastal plain
694 has resulted in the development of groundwater depression cones from Zaoyuan well field to Fangezhuang,
695 with the aggravation of seawater intrusion in this region. In the 1950s, the seawater intrusion in the study
696 area was only occurred within 2 km distance from the coastline, and it expanded to over 5 km distance in
697 the 1980s. In 1986, the groundwater depression cone centered in the Zaoyuan well field was characterized
698 by 6 meters depths below the sea level, with the water level 3 m.a.s.l. The enclosed area by 0 m.a.s.l water
699 level contours covered 10 km². The original $\text{Ca}-\text{HCO}_3$ type water changed to $\text{Ca}-\text{Na}-\text{Cl}$ type. Apart from
700 the intensive exploitation fresh groundwater from coastal aquifer, the successive drought (1976–1989) also
701 played important roles on controlling the groundwater recharge and exacerbating seawater intrusion in the
702 coastal area of north China (Wilhite, 1993; Han et al., 2015). In this study area, the annual mean
703 precipitation was 668.7 mm during 1954–1995, the Cl concentrations was ranging from 130 to 170 mg/L in
704 the Zaoyuan well field. Whereas the annual mean precipitation reduced to 559.7 mm during 1996–2011,
705 resulting in Cl concentration in the well field up to 550 mg/L in May 1986, and 812 mg/L in July 2006. It
706 has seriously threatened the safety of water supply in this region. The seawater intrusion in the coastal
707 aquifer shows the wedge-shaped body and has vertically characterized by freshwater in the upper part and
708 salt water in the lower part of shallow aquifer. Since 2002, with the establishment of anti-tide dam in the
709 Yangtze River estuary area, it has good effect on preventing the horizontal pouring seawater into riverway.

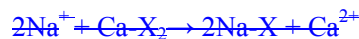
710 Thus, the seawater intrusion is mainly caused by lateral inflow of seawater in the aquifer.

711 According to the guidelines of drinking water standards from China Environmental Protection
712 Authority (GB 5749-2006) or US EPA or WHO, the guideline of chloride concentration for drinking water
713 is 250 mg/L. Most groundwater distributed in the seawater intrusion area cannot be used for irrigation, the
714 source of drinking water and industrial utilization. It has enhanced the scarcity of fresh water resources in
715 this region by vicious cycle of groundwater level decline → seawater intrusion → groundwater salinization
716 → groundwater level decline again. This will also influence the surface water runoff. How to judge the
717 criterion of seawater intrusion? Generally, 250 mg Cl/L can be regarded as the intruded standard, and more
718 than 1000 mg Cl/L as the serious intrusion (Jiang and Li, 1997; Zhuang et al., 1999). Some studies took the
719 TDS (>1000 mg/L) as the intruded standard (e.g., Xue et al., 1997; Zhang and Peng, 1998). Water type can
720 also be used as the intruded standard, such as Ca-Cl type water occurs during seawater intrusion into
721 freshwater aquifers, and Na-HCO₃ type water displays during flushing of the mixing zone by freshwater
722 (Appleo and Postma, 1993). Additionally, the multi-hydrochemical ionic ratios can also provide important
723 confirmation of hydrogeochemical processes modifying groundwater chemistry during seawater intrusion
724 (Vengosh et al., 1997; Jones et al., 1999). However, the frequent anthropogenic activities modified coastal
725 hydrologic dynamics and hydrogeochemical characteristics to great extent. For instance, with except of
726 modern seawater, the sources of chloride in groundwater system could be derived from paleoseawater relics
727 in aquifers, infiltration of agricultural return flow with fertilizer solutions, and discharge of industrial and
728 domestic wastewater.

729 Hydrogeochemical facies evolution diagram (HFE-D) proposed by Giménez-Forcada (2010) can be
730 used to analyze the phase of seawater intrusion or freshening and its dynamics. From Fig. 8, it can be seen
731 that most brackish groundwaters (e.g., G11, G16, G17, G20, G25, G28, G29) have evolved in the series of
732 Ca-HCO₃ → Ca-Cl → Na-Cl facies under the intrusion period. Locally, several water samples (e.g., G1,
733 G12, G26) collected from the interfluvial area have been characterized by freshening process. Deep
734 groundwater G11 sampled from the well field shows being under salinizing period in the relatively dry
735 season, and under freshening period in the relatively wet season. In the coastal zone, the river water has
736 obvious mixing trend between end members. Some shallow groundwaters (e.g., G2, G4, G10, G13, G15)
737 are close to the mixing line between end members on this figure, indicating significant mixing with
738 seawater. The groundwaters (G10, G11, G15, G26) collected from the productive wells of the Zaoyuan
739 well field display the different processes occurring in salinizing or freshening stages, indicating that the

740 heterogeneous hydrogeological conditions could be responsible for this distinguished patterns.

741 The calculated results of saturated indices (Fig. 9) show that that SI_{cal} and SI_{dol} have some deviation
742 from equilibrium (−0.4 to +0.5 for SI_{cal} , and −0.5 to +0.5 for SI_{dol}). The distribution of SI_{cal} and SI_{dol} is
743 related to the sampling period. In the wet season, most of water samples are characterized by $SI_{\text{cal}} < 0$ and
744 $SI_{\text{dol}} < 0$, suggesting they are under unsaturated for these minerals, while in the dry season, most of water
745 samples are under saturated with respect to these minerals. In contrast, all sampled groundwater had
746 negative saturation indices with respect to gypsum ($SI_{\text{gyp}} < 0$), indicating that these water samples are
747 under saturated with respect to gypsum. The plots (Fig. 10 a-f) of ionic molar ratios (Na/Cl , SO_4/Cl , Mg/Ca ,
748 $\text{Ca}/(\text{SO}_4+\text{HCO}_3)$, Ca/SO_4 , and $(\text{Ca}+\text{Mg})/\text{Cl}$) can be used to further reveal the groundwater salinized
749 processes and dominated hydrochemical behavior. The brackish groundwaters in this study area have an
750 enriched Ca^{2+} (i.e., the ratio of $\text{Ca}/(\text{HCO}_3+\text{SO}_4) > 1$ with low ratios of Na/Cl and SO_4/Cl as the seawater
751 proportion in the mixture increases. As shown in Fig. 10a, Na/Cl ratios of brackish groundwater affected by
752 seawater intrusion are usually lower than the ratio (0.86) of modern seawater. The high Na/Cl ratios (>1)
753 could be typical of anthropogenic sources (i.e., domestic waste waters). When seawater intrudes into
754 coastal freshwater aquifers, Ca^{2+} on the clay bearing sediments can be replaced by Na^+ :



755 This process can decrease the Na/Cl ratios and increase the $(\text{Ca}+\text{Mg})/\text{Cl}$ ratios. The dolomitization
756 process can be described by the transformation reaction (Appelo and Postma, 2005):



757 It can result in Ca enrichment over Mg in solution and that Mg/Ca ratios decreases. This process may
758 also be characterized by Ca-Cl water type.

759 To explain the enrichment in Ca^{2+} relative to SO_4^{2-} concentrations, observed in most water samples
760 (Fig. 10e), gypsum dissolution ($SI_{\text{gyp}} < 0$) can be coupled by cation exchange reactions under the interaction
761 with clay stratum and calcite precipitation with incongruent dissolution of dolomite and gypsum.
762 Additionally, due to the ORP values ranging from 3 to 74 mV for 18 of 22 water samples collected in
763 August 2010, the sulfate reduction under anaerobic conditions may be responsible for relatively high
764 Ca/SO_4 and low SO_4/Cl ratios. Generally, low Na/Cl , SO_4/Cl and high $\text{Ca}/(\text{HCO}_3+\text{SO}_4) (>1)$ ratios are
765 further indicator of the arrival of seawater intrusion.

766 ΔNa is negative in most samples of this area (Fig. 11a and Fig. 12a). The depletion of Na^+ could be
767 caused by the inverse cation exchange taken place with the clay sediments. This exchange produces Ca

770 release to the solution during the seawater intrusion. The positive ΔCa and ΔMg may be due to the
771 dissolution of calcite, dolomite and gypsum present in the aquifer strata. Water flushing during aquifer
772 recharge can result in positive ΔNa and negative ΔCa and/or ΔMg (Fig. 11a). For some water samples, the
773 Ca enrichment is not accompanied by Na depletion, which could be caused by dolomitization (Ca
774 enrichment with Mg depletion) (Fig. 12b). The excess of SO_4^{2-} compared to conservative mixing (Fig. 11d)
775 can be explained by redissolution of the precipitated gypsum along the mixing front.

776 **5.2.2 Mixing between thermal and cold groundwater**

777 Sea level rose by about 100 m since the end of the last glacial period (18,000 years, 18 ka BP) and
778 stabilized around 5 ka BP in the eastern China (Yang, 1996). The marine sediments could not be found in
779 the geothermal field, indicating the transgression in the geologic history did not occur around Danihe area
780 (Zeng, 1991). However, the fracture and structural fissure developed well in this study area became the
781 major subsurface pathway of seawater intrusion. The previous studies have revealed that the geothermal
782 waters in this area are characterized by the features of residual seawater and modern precipitation (Zeng,
783 1991; Hui, 2009). The results of ^{14}C age dating for the geothermal waters in this area are ranging from 3.4
784 ka to 12.8 ka with lower tritium contents (less than 2 TU) (Zeng, 1991). The Piper plot (Fig. 5) shows
785 CaNa-Cl type water for the geothermal waters. It is noteworthy that the geothermal water from Danihe
786 geothermal field has higher Sr concentrations (up to 89.8 mg/L) relative to that in seawater (5.4–6.5 mg/L in
787 this study), due to the Sr bearing minerals (i.e., celestite, strontianite) with Sr contents of 300–2000 mg/kg
788 present in the bedrock (Hebei Geology Survey, 1987). The mixture waters sampled from the geothermal
789 field in this study also have the higher Sr concentrations relative to seawater, i.e., G9 with Sr concentrations
790 ranging from 7.4 to 11.6 mg/L, and G19 from 4.9 to 7.1 mg/L. The diagram of chloride versus strontium
791 concentrations of different water samples (Fig. 13) shows that the groundwater samples (e.g., G9, G19)
792 collected from the geothermal field have obviously been characterized by closing to mixing line between
793 fresh cold and thermal groundwater. Some waters (G16, G20, G29) sampled from the downstream area
794 also close to this mixing line, indicating the thermal water overflows into the coastal aquifers in different
795 depths. The water samples collected from the well field are located between two mixing lines (Fig. 13),
796 suggesting the groundwater in the well field simultaneously suffered from the mixing with thermal water
797 and obvious seawater intrusion. Additionally, the points of water samples (G5, G8, G9, and G19), collected
798 from the geothermal field, mainly occurs on the HFE D (Fig. 8) in the 1/2 (MixCa-Cl) and 1/6 (Ca-Cl) facies
799 zones, indicating these waters have been modified by the reverse base exchange reactions.

As both Cl and Br are not affected by water-rock interactions and usually behave conservatively, the Cl/Br ratio can be used as a reliable tracer to study the processes of evaporation and salinization of water (Edmunds, 1996; Jones et al., 1999). Standard seawater (Cl/Br molar ratio=650.8) may be distinguished from relies of evaporated seawater (normally less than 669.3), input of evaporite dissolution (more than 2256) and anthropogenic pollution (e.g., sewage effluents, Cl/Br ratios up to 1805; Vengosh and Pankratov, 1998) or agricultural return flows with low Cl/Br ratios (Jones et al., 1999). It can be seen from Fig. 14 that the points of the thermal waters lie lower than the ratio line of standard seawater, indicating that they are affected by mixing with relies of evaporated seawater. The points of cold groundwaters (G9, G19) sampled from the geothermal field display between the seawater and the thermal waters, indicating these cold waters are mixture between cold groundwater and the thermal water, which has relies of evaporated seawater. However, it cannot exclude adding the Br inputs into groundwater system through the pesticides application of the pronounced agricultural activity (Davis et al., 1998), this effect could lower the Cl/Br ratios of the groundwaters. The groundwater sample G10 in the well field shows the feature of high Cl/Br ratio in Fig. 14, indicating obvious anthropogenic inputs (e.g., discharge domestic wastewater) occurring in the shallow aquifers around the well field.

5.2.3 Interaction between surface and ground water

Coastal zones encompass the complex interaction among different waters (i.e., river water, seawater, groundwater, rainfall water). The interaction between surface and ground water in the Yang-Dai River coastal plain is usually ignored by the previous studies. However, understanding how surface water interacts with the groundwater is essential for managing freshwater resources. Groundwater depression cone below the sea level has formed in the early 1980s. Due to the irrigation supported by transfer of surface water from the upper and middle stream of Yang-Dai River, the amount of surface water discharged into the Bohai Sea declined to great extent. Under the tide effects, seawater can be poured into the estuary of the downstream section of the rivers, resulting in the river bed filled with saltwater, which can cause mixing between river water and seawater. The results of water chemistry analysis from two river sections show that the distribution of salt water reached more than 10 km above the estuary of the Yang River, and about 4 km above the estuary of the Dai River (Han, 1988). It led to that the seawater simultaneously intruded into the coastal aquifers through not only the lateral subsurface flow from coastline to the inland but also vertical infiltration from the riverbed to both sides of the river. The hazard caused by the latter pattern had been more serious than the former pattern, before the establishment of anti-tide dam at the

830 estuary of Yang River. Currently, the seawater intruded distance towards inland has been controlled within
831 4 km away from the coastline.

832 The stable isotope compositions of different water samples (Fig. 4) display that the points of most
833 surface water samples are deviated from the LMWL to the right, indicating that these waters are likely to be
834 subject to evaporation to different degrees. The points of surface water samples (S1, S2, S3, and S7) in
835 Fig. 4 close to the compositions of local seawater, indicating the pronounced mixing process with seawater
836 for these surface waters. However, the samples S2, S6, S8, and S9 have the depleted compositions of stable
837 isotopes, probably resulting from the exchange between them and local groundwater. S12, located at the
838 estuary area, has variable compositions due to the sampling seasons. HFE-D shows that most of surface
839 water samples are close to the mixing line between end members (freshwater and seawater). S9 is
840 significantly characterized by salinization process probably due to the interaction with ambient
841 groundwater. It can be seen from the relationship between ionic delta values and seawater proportions for
842 the water samples (Fig. 11) that G1, G11, G12, G14', G26, G29, due to these wells close to the river or
843 located at the flat interfluvium, may be dominated by the obvious freshening process. While G2, G3, and G16
844 under the salinizing process could be subject to the vertical infiltration of saltwater in the river. The points
845 of surface waters (S1, S2, S3, and S7) on Fig. 4 and Fig. 8 are distributed along the mixing line between
846 fresh and sea water end members. It is due to the direct mixture occurs in the riverway. S12 sampled from
847 the Dai River estuary may be contaminated by the wastewater discharge with higher Sr concentration
848 relative to seawater. By contrast, surface water from the Dai River have higher seawater proportions
849 compared with that from Yang River, owing to that the local government did not establish anti tide dam in
850 the Dai River estuary. G1, G2, G3, G10 and G13 collected from coastal zone are obviously mixed with
851 seawater with closing to the mixing line between seawater and freshwater in Fig. 13.

852 5.3-4 Conceptual model of groundwater flow patterns, salinization and management
853 implications

854 Generally, groundwater in this study area is mainly originated from precipitation, river
855 infiltration, lateral subsurface runoff, upflow of geothermal waters and seawater intrusion in
856 the coastal area. The associated hydrological processes driven by the natural (hydrologic,
857 geologic, climatic) changes and anthropogenic activities have resulted in groundwater
858 salinization processes, along with the complex hydrogeochemical characteristics of
859 groundwater system. Groundwater changes from Ca-HCO₃ type water in the piedmont area to
860 the Na-Cl type water in the coastal area.

861 Coastal zones encompass the complex interaction among different water bodies (i.e., river water,

seawater and groundwater). The interactions between surface- and ground-water in the Yang-Dai River coastal plain have generally been ignored in previous studies. However, the surface water chemistry data show that the distribution of salt water has historically reached more than 10 km inland along the estuary of the Yang River, and approximately 4 km inland in the Dai River (Han, 1988). The relatively higher proportion of seawater-intrusion derived salinity in shallow samples in this study, along with the evidence from resistivity surveys (Fig. X6; Zuo, 2006) indicate that intrusion by vertical leakage from these estuaries is therefore an important process. The hazard associated with this pathway in recent times has been reduced by the construction of a tidal dam, which now restricts seawater ingress along the Yang estuary to within 4 km of the coastline. This may alleviate salinization to an extent in future in the shallow aquifer by removing one of the salinization pathways, however, as described, there are multiple other salinization processes impacting the groundwater in the Quaternary aquifers of the region.

A conceptual model of the groundwater flow system in the Yang-Dai River coastal plain ~~can be~~ is summarized in Fig. 15.122. This model presents an advance on the previous understanding of the study area, by delineating ~~four~~ four subsurface major processes responsible for groundwater salinization in this area. These are: 1. ~~including~~ Seawater intrusion by lateral sub-surface flow; 2. Interaction between saline surface water and groundwater (e.g. vertical leakage of saline water from the river estuaries); 3. ~~return flow of agricultural irrigation, mixing with between low-temperature groundwater and deep~~ geothermal water; and, 4. Irrigation return-flow and associated anthropogenic contamination ~~interaction~~ between surface water and groundwater/seawater, could be responsible for the groundwater salinization in this area. Both the lateral and vertical intrusion of saline water are driven by the long-term over-pumping of groundwater from fresh aquifers in the region. The ~~Two aspects of seawater intrusion, identified by depleted ΔNa and enriched ΔCa with Ca/Cl type water and Ca/(HCO₃+SO₄)>1 and lower Na/Cl and SO₄/Cl relative to these ratios of seawater, can be delineated, namely vertical infiltration of saltwater inflow towards the inland estuary and lateral inflow of seawater driven by over pumping groundwater from fresh aquifers. Irrigation return-flow from local groundwater agriculture can results from over-irrigation of crops, and is responsible for cause groundwater extensive~~ nitrate pollution (up to 340 mg/L NO₃⁻ in groundwater of this area) ~~due to the infiltration and probably due to~~ dissolution of fertilizers ~~during infiltration. The somewhat enriched stable isotopes in shallow groundwater (more pronounced in the dry season) also indicate that such return-flow may recharge water impacted by evaporative salinization into the aquifer. The geothermal water, with distinctive chemical composition (e.g. depleted stable isotopes, high TDS,~~ 30

892 Ca, F, and Sr concentrations), is also demonstrated in this study to be a significant contributor to
893 groundwater salinization, via upward mixing. The study area is therefore in a situation of unusual
894 vulnerability, in the sense that it faces salinization threats simultaneously from lateral, downward and
895 upward migration of saline water bodies.

896 According to drinking water standards and guidelines from China Environmental Protection Authority
897 (GB 5749-2006) and/or US EPA and WHO, chloride concentration in drinking water should not exceed 250
898 mg/L. At the salinity levels observed in this study - many samples impacted by salinization
899 contain >500mg/L of chloride (Table 1) - a large amount of groundwater is now or will soon be unsuitable
900 for domestic usage, as well as irrigation or industrial utilization. So far, this has enhanced the scarcity of
901 fresh water resources in this region, leading to a cycle of groundwater level decline → seawater intrusion
902 → loss of available freshwater → increased pumping of remaining fresh water. If this cycle continues, it is
903 likely to further degrade groundwater quality and restrict its usage in the future. Such a situation is typical
904 of the coastal water resources 'squeeze' highlighted by Michael et al., (2017). Alternative management
905 strategies, such as restricting water usage in particular high-use sectors, such as agriculture, industry or
906 tourism, that are based on a comprehensive assessment of the social, economic and environmental benefits
907 and costs of these activities, warrants urgent and careful consideration.

908 —flows into the Quaternary aquifers, mixing with cold groundwater, and transports to the downstream
909 area of Yang River Basin. Additionally, the interaction between surface and ground water can cause
910 seasonal flushing local groundwater in the upstream interfluve or lead to saltwater infiltration affected by
911 tide/surge along the riverbed at the estuary.

912 **6. Conclusions**

913 It has been recognized that groundwater in the Quaternary aquifers of the Yang-Dai River coastal
914 plain is the an important water resource for agricultural irrigation, urban and domestic use (including for
915 tourism) —tourism development and industrial utilization activity. Natural climate change (e.g., continuous
916 drought, overflow of geothermal water) and Extensive groundwater utilization human activities have has
917 made the problem of groundwater salinization in this area increasingly prominent, even resulting in the
918 closure of the Zaoyuan well fieldwells in the area. Based on the analysis of hydrochemical and stable
919 isotopic compositions of different water bodies, including surface water, cold groundwater, geothermal
920 water, and seawater, we delineated the key groundwater flow system and groundwater salinization

921 processes. Seawater intrusion is the main aspect process responsible for the groundwater salinization in the
922 coastal zone; however this likely includes ing the vertical saltwater infiltration along the riverbed into
923 aquifers, which is affected by the tide/surge process, and as well as the lateral seawater intrusion caused by
924 pumping for fresh groundwater at the Zaoyuan wellfield. The overflow upward mixing of the highly
925 mineralized thermal water into the Quaternary aquifers along the fault zone mixes with the cold
926 groundwater and makes it salinized is also evident, particularly through the use of stable isotope, chloride
927 and strontium end-member mixing analysis. Additionally, significant The thermal water has characterized
928 by lower Cl/Br ratios and higher Sr concentrations relative to seawater. It cannot be ignored that the
929 salinization or nitrate pollution from the anthropogenic activities (e.g., agricultural irrigation return-flow
930 with dissolution of fertilizers) and locally, intrusion of heavily polluted seawater, are also evident.
931 Additionally, the interaction between surface and ground water can also affect the groundwater
932 salinization in this area. Different approaches of hydrochemical analysis, such as Piper plot, HFE D, major
933 ionic ratios (Na/Cl, SO₄/Cl, Ca/SO₄, (Ca+Mg)/Cl, Ca/(SO₄+HCO₃), Cl/Br) and Sr, were used in this study
934 to identify the different hydrogeochemical reactions and freshening or salinizing processes in the
935 Quaternary aquifers.

936

937 Groundwater salinization has become a prominent water environment problem in the coastal areas of
938 northern China (Han et al., 2014; Han et al., 2015; Han et al., 2016a), which has caused the and threatens to
939 create further paucity of fresh water resources, which may prove a significant impediment to further social
940 and economic and has become the bottleneck of urban development in these regions to a certain extent.
941 Since the 1990s, the local government has begun to pay attention to the development problem of seawater
942 intrusion, and the irrational exploitation of groundwater has been restricted in some cases. The Zaoyuan
943 well field has ceased to pump groundwater since 2007, while an The anti-tide dam (designed to protect
944 against tidal surge events) has been established in the Yang River estuary area in 2002, may also reduce
945 saline intrusion effectively intercepting the seawater pouring into riverway during the tide/surge period in
946 future. However, due to the significant lag-time associated with groundwater systems, a response in terms
947 of water quality may take time to emerge, and in the meantime the other salinization and pollution impacts
948 documented here may continue to threaten water quality. These actions have made the rate of intrusion
949 slowed down. The joint use of surface water and groundwater with reasonable exploitation program is
950 essential and economical for the local water resources management. In this regard, we recommend However,

951 the quantitative understanding to the vertical and lateral saltwater intrusion into fresh aquifers continued
952 monitoring of groundwater quality and levels, and active programs to reduce input of anthropogenic
953 contaminants such as nitrate from fertilizers, and appropriate well-construction and decommissioning
954 protocols to prevent contamination through preferential pathways.

955 ~~should be obtained from further continuous groundwater monitoring and numerical groundwater flow
956 and transport modeling. This study would be benefit the local agricultural development and groundwater
957 resources management.~~

958 Acknowledgement

959 This research was supported by Zhu Kezhen Outstanding Young Scholars Program in the Institute of
960 Geographic Sciences and Natural Resources Research, Chinese Academy of Sciences (CAS) (grant number
961 2015RC102), and Outstanding member program of the Youth Innovation Promotion Association, CAS
962 (grant number 2012040). The authors appreciate the helpful field work and data collection made by Mr
963 Yang Jilong from Tianjin Institute of Geology and Mineral Resources, Dr. Wang Peng and Dr Liu Xin from
964 Chinese Academy of Sciences.

965

966 References

967 An T.D., Tsujimura M., Phu V.L., Kawachi A., Ha D.T., 2014. Chemical Characteristics of Surface Water
968 and Groundwater in Coastal Watershed, Mekong Delta, Vietnam. The 4th International Conference on
969 Sustainable Future for Human Security, SustaiN 2013. Procedia Environmental Sciences. 20:712-721.
970 Andersen, M.S., Jakobsen, V.N.R., Postma, D. 2005. Geochemical processes and solute transport at the
971 seawater/freshwater interface of a sandy aquifer. Geochimica et Cosmochimica Acta. 69(16):
972 3979-3994.

973 Appelo C. A. J., Postma D., 1993. Geochemistry, Groundwater and Pollution, first edition. A. A. Balkema,
974 Brookfield, Vt.

975 Appelo C.A.J., 1994. Cation and proton exchange, pH variations, and carbonate reactions in a freshening
976 aquifer. Water Resour. Res., 30, 2793-2805.

977 Appelo C.A.J., Postma D., 2005. Geochemistry, Groundwater and Pollution, second edition. Taylor &
978 Francis Group.

979 Bao J., 2005. Two-dimensional numerical modeling of seawater intrusion in Qinhuangdao Region. Master's
980 Thesis. Tongji University, Shanghai, China. (Chinese with English abstract)

981 Barbicot F., Marlin C., Gibert E., Dever L., 2000. Hydrochemical and isotopic characterisation of the
982 Bathonian and Bajocian coastal aquifer of the Caen area (northern France). Applied Geochemistry.
983 15:791-805.

984 Bobba A.G., 2002. Numerical modelling of salt-water intrusion due to human activities and sea-level
985 change in the Godavari Delta, India. Hydrological Sciences. 47(S), S67-S80.

986 Bobba A.G., 2002. Numerical modelling of salt-water intrusion due to human activities and sea-level
987 change in the Godavari Delta, India. Hydrological Sciences. 47(S), S67-S80.

988 Bouchaou L., Michelot J.L., Vengosh A., Hsissou Y., Qurtobi M., Gaye C.B., Bullen T.D., Zuppi G.M.,
989 2008. Application of multiple isotopic and geochemical tracers for investigation of recharge,

990 salinization, and residence time of water in the Souss–Massa aquifer, southwest of Morocco. *Journal*
991 of *Hydrology*. 352: 267-287.

992 Brockway R., Bowers D., Hoguane A., Dove V., Vassele V., 2006. A note on salt intrusion in funnel-shaped
993 estuaries: Application to the Incomati estuary, Mozambique. *Estuarine, Coastal and Shelf Science*.
994 66:1-5.

995 Cary L., Petelet-Giraud E., Bertrand G., Kloppmann W., Aquilina L., Martins V., Hirata R., Montenegro S.,
996 Pauwels H., Chatton E., Franzen M., Aurouet A., the Team. Origins and processes of groundwater
997 salinization in the urban coastal aquifers of Recife (Pernambuco, Brazil): A multi-isotope approach.
998 *Science of the Total Environment*. 530-531:411-429.

999 Chen M., Ma F., 2002. Groundwater resources and the environment in China. Seismological Press. Beijing.
1000 pp255-281. (in Chinese)

1001 Craig, H., 1961. Standard for reporting concentration of deuterium and oxygen-18 in natural water. *Science*
1002 133, 1833–1834.

1003 Creel L., 2003. Ripple effects: Population and coastal regions. Population Reference Bureau. pp1-7.<
1004 <http://www.prb.org/Publications/Reports/2003/RippleEffectsPopulationandCoastalRegions.aspx>>

1005 [Currell M.J., Cartwright, I., Bradley, D.C., Han, D.M., 2010. Recharge history and controls on groundwater](#)
1006 [quality in the Yuncheng Basin, north China. Journal of Hydrology](#). 385: 216-229.

1007 [Currell M.J., Dahlhaus P.D., Ii H. 2015. Stable isotopes as indicators of water and salinity sources in a](#)
1008 [southeast Australian coastal wetland: identifying relict marine water, and implications for future](#)
1009 [change. Hydrogeology Journal](#). 23: 235-248.

1010 [Currell M.J., Han D. 2017. The Global Drain: Why China's water pollution problems should matter to the](#)
1011 [rest of the world. Environment: Science and Policy for Sustainable Development](#). 59(1): 16-29.

1012 de Montety V., Radakovitch O., Vallet-Coulob C., Blavoux B., Hermitte D., Valles V., 2008. Origin of
1013 groundwater salinity and hydrogeochemical processes in a confined coastal aquifer: Case of the Rhône
1014 delta (Southern France). *Applied Geochemistry*. 23: 2337-2349.

1015 Edmunds W. M., 1996. Bromine geochemistry of British groundwaters. *Mineral. Mag.*, 60, 275–284.

1016 El Yaouti F., El Mandour A., Khattach D., Benavente J., Kaufmann O., 2009. Salinization processes in the
1017 unconfined aquifer of Bou-Areg (NE Morocco): A geostatistical, geochemical, and tomographic study.
1018 *Applied Geochemistry*. 24:16-31.

1019 Ferguson G., Gleeson T., 2012. Vulnerability of coastal aquifers to groundwater use and climate change.
1020 *Nature Climate Change*. 2, 342-345.

1021 Fidelibus M.D., Giménez E., Morell I., Tulipano L., 1993. Salinization processes in the Castellon Plain
1022 aquifer (Spain). In: Custodio, E., Galofré, A. (Eds.), *Study and Modelling of Saltwater Intrusion into*
1023 *Aquifers*. Centro Internacional de Métodos Numéricos en Ingeniería, Barcelona, pp267-283.-

1024 Garing C., Luquot L., Pezard P.A., Gouze P., 2013. Geochemical investigations of saltwater intrusion into
1025 the coastal carbonate aquifer of Mallorca, Spain. *Applied Geochemistry*. 39:1-10.

1026 Ghassemi F., Chen T.H., Jakeman A.J., Jacobson G., 1993. Two and three-dimensional simulation of
1027 seawater intrusion: performances of the “SUTRA” and “HST3D” models. *AGSO J.*
1028 *Aust.Geol.Geophys*. 14(2-3):219-226.

1029 Ghiglieri G., Carletti A., Pittalis D., 2012. Analysis of salinization processes in the coastal carbonate aquifer
1030 of Porto Torres (NW Sardinia, Italy). *Journal of Hydrology*. 432-433:43-51.

1031 Giambastiani B.M.S., Antonellini M., Oude Essink G.H.P., Stuurman R.J., 2007. Saltwater intrusion in the
1032 unconfined coastal aquifer of Ravenna (Italy): A numerical model. *Journal of Hydrology*. 340:91-104.

1033 Giménez-Forcada E., 2010. Dynamic of sea water interface using hydrochemical facies evolution diagram,

1078 | [coastal aquifer: Evidence from groundwater isotopes, and environmental significance. Science of the](#)
1079 | [Total Environment. 544: 995-1007](#)

1080 Masterson J.P., 2004. Simulated interaction between freshwater and saltwater and effects of ground-water
1081 pumping and sea-level change, Lower Cape Cod aquifer system, Massachusetts: U.S. Geological
1082 Survey Scientific Investigations Report 2004-5014, 72 p.

1083 Mazi, K., Koussis, A.D., Destouni, G., 2014. Intensively exploited Mediterranean aquifers: proximity to
1084 tipping points and control criteria for sea intrusion. *Hydrol. Earth Syst. Sci.* 18, 1663-1677.

1085 Meng F., 2004. Rational development of groundwater resources on the coastal zone of Qinhuangdao area.
1086 *Marine Geology Letters.* 20(12):22-25. (Chinese with English abstract)

1087 | [Michael H.A., Post V.E.A., Wilson A.M., Werner A.D. 2017. Science, society and the coastal groundwater](#)
1088 | [squeeze. Water Resources Research. 53. 2610-2617.](#)

1089 Mondal N.C., Singh V.P., Singh V.S., Saxena V.K., 2010. Determining the interaction between groundwater
1090 and saline water through groundwater major ions chemistry. *Journal of Hydrology.* 388:100-111.

1091 Montenegro S.M.G., de A. Montenegro A.A., Cabral J.J.S.P., Cavalcanti G., 2006. Intensive exploitation
1092 and groundwater salinity in Recife coastal plain (Brazil): monitoring and management perspectives.
1093 *Proceedings 1st SWIM-SWICA Joint Saltwater Intrusion Conference, Cagliari-Chia Laguna, Italy -*
1094 *September 24-29, 2006.* pp79-85.

1095 Moore W.S., 1996. Large groundwater inputs to coastal waters revealed by ^{226}Ra enrichments. *Nature*
1096 380,612-214.

1097 Narayan K.A., Schleeberger C., Bristow K.L., 2007. Modelling seawater intrusion in the Burdekin Delta
1098 Irrigation Area, North Queensland, Australia. *Agricultural Water Management.* 89:217-228.

1099 Pan G, Yang Y., Zhang L., 1990. Survey report of geothermal water in Qinhuangdao city of Hebei Province.
1100 Team of mineral hydrological and engineering geology from the Bureau of Geology and mineral
1101 Resources of Hebei Province, China. (in Chinese)

1102 Parkhurst D.L., Appelo C.A.J., 1999. User's Guide to PHREEQC – A Computer Program for Speciation,
1103 Reaction-Path, 1D-Transport, and Inverse Geochemical Calculation. US Geol. Surv. Water-Resour.
1104 Invest. Rep. 99-4259.

1105 Post V.E.A., 2005. Fresh and saline groundwater interaction in coastal aquifers: Is our technology ready for
1106 the problems ahead? *Hydrogeology Journal.* 13:120-123.

1107 Price R.M., Herman J.S., 1991. Geochemical investigation of salt-water intrusion into a coastal carbonate
1108 aquifer: Mallorca, Spain. *Geological Society of America Bulletin.* 103:1270-1279.

1109 Pulido-Leboeuf P., 2004. Seawater intrusion and associated processes in a small coastal complex aquifer
1110 (Castell de Ferro, Spain). *Applied Geochemistry.* 19:1517-1527.

1111 Radhakrishna I., 2001. Saline fresh water interface structure in Mahanadi delta region, Orissa, India.
1112 *Environmental Geology.* 40(3):369-380.

1113 Rahmawati N., Vuillaume J., Purnama I.L.S., 2013. Salt intrusion in Coastal and Lowland areas of
1114 Semarang City. *Journal of Hydrology.* 494:146-159.

1115 Robinson M.A., Gallagher D.L., Reay W.G., 1998. Field observations of tidal and seasonal variations in
1116 ground water discharge to estuarine surface waters. *Ground Water Monitoring and Remediation.* 18
1117 (1): 83-92.

1118 Shen Z., Zhu Y., Zhong Z., 1993. Theoretical basis of hydrogeochemistry. Geological Publishing House.
1119 Beijing, China. (in Chinese)

1120 Sherif M.M., Singh V.P., 1999. Effect of climate change on sea water intrusion in coastal aquifers.
1121 *Hydrological Processes* 13, 8:1277-1287.

1122 Shi M.Q., 2012. Spatial distribution of population in the low elevation coastal zone and assessment on
1123 vulnerability of natural disaster in the coastal area of China. Master thesis of Shanghai Normal
1124 University, 24–32.(Chinese with English abstract)

1125 Simpson, M.J., Clement, T.P., 2004. Improving the worthiness of the Henry problem as a benchmark for
1126 density-dependent groundwater flow models. *Water Resources Research* 40 (1), W01504
1127 doi:10.1029/2003WR002199.

1128 Sivan O., Yechieli Y., Herut B., Lazar B., 2005. Geochemical evolution and timescale of seawater intrusion
1129 into the coastal aquifer of Israel. *Geochimica et Cosmochimica Acta*. 69(3):579-592.

1130 Smith A.J., Turner J.V., 2001. Density-dependent surface water-groundwater interaction and nutrient
1131 discharge in the Swan-Canning Estuary. *Hydrological Processes*. 15:2595-2616.

1132 SOA (State Oceanic Administration of the People's Republic of China), 2015. China's Marine Environment
1133 Bulletin: 2014. Released 11th March, (in Chinese).

1134 Sophocleus M., 2002. Interactions between groundwater and surface water: the state of science.
1135 *Hydrogeology Journal*. 10:52-67.

1136 Sun J., Yang Y., 2007. Seawater intrusion characteristics in Qinhuangdao. *Journal of Environmental
1137 Management College of China*. 17(2):51-54. (Chinese with English abstract)

1138 UN Atlas, 2010. UN Atlas: 44 Percent of us Live in Coastal Areas.
1139 <<http://coastalchallenges.com/2010/01/31/un-atlas-60-of-us-live-in-the-coastal-areas/>>.

1140 Vengosh A., Gill J., Reyes A., Thoresberg K., 1997. A multi-isotope investigation of the origin of ground
1141 water salinity in Salinas Valley, California. *American Geophysical Union*, San Francisco, California.

1142 Vengosh A., Pankratov I., 1998. Chloride/bromide and chloride/fluoride ratios of domestic sewage effluents
1143 and associated contaminated ground water. *Ground Waer*. 36(5):815-824.

1144 [Vengosh A., Spivack A.J., Artzi Y., Ayalon A. 1999. Geochemical and boron, strontium, and oxygen
1145 isotopic constraints on the origin of the salinity in groundwater from the Mediterranean coast of Isreal.
1146 Water Resources Research](#). 35(6): 1877-1894.

1147 [Walraevens, K., Cardenal-Escarcena, J., Van Camp, M., 2007. Reaction transport modelling of a freshening
1148 aquifer \(Tertiary Ledo-Paniselian Aquifer, Flanders-Belgium\). Applied Geochemistry](#). 22: 289-305.

1149 Wang J., Yao P., Bianchi T.S., Li D., Zhao B., Cui X., Pan H., Zhang T., Yu Z., 2015. The effect of
1150 particle density on the sources, distribution, and degradation of sedimentary organic carbon in the
1151 Changjiang Estuary and adjacent shelf. *Chemical Geology*. 402:52-67.

1152 [Weber, K., Stewart, M., 2004. A critical analysis of the cumulative rainfall departure concept. Ground
1153 Water](#) 42 (6), 935–938.

1154 Werner A.D., 2010. A review of seawater intrusion and its management in Australia. *Hydrogeology Journal*.
1155 18(1):281-285.

1156 Werner A.D., Bakker M., Post V.E.A., Vandenbohede A., Lu C., Ataie-Ashtiani B., Simmons C.T., Barry
1157 D.A., 2013a. Seawater intrusion processes, investigation and management: Recent advances and
1158 future challenges. *Advances in Water Resources*.51:3-26.

1159 Werner A.D., Simmons C.T., 2009. Impact of sea-level rise on seawater intrusion in coastal aquifers.
1160 *Ground Water*. 47:197-204.

1161 Westbrook S.J., Rayner J.L., Davis G.B., Clement T.P., Bjerg P.L., Fisher S.J., 2005. Interaction between
1162 shallow groundwater, saline surface water and contaminant discharge at a seasonally and tidally forced
1163 estuarine boundary. *Journal of Hydrology*, 302:255-269.

1164 Wilhite D.A., 1993. *Drought Assessment, Management, and Planning: Theory and Case Studies*. Springer U
1165 S. p628.

1166 Xu G., 1986. Analysis of seawater intruding into aquifer system in Beidaihe Region. *Hydrogeology &*
1167 *Engineering Geology*. 2:7-10. (in Chinese)

1168 Xue Y., Wu J., Xie C., Zhang Y., 1997. Study of seawater and saltwater intrusion in the coast plain of
1169 Laizhou Bay. *Chinese Science Bulletin*. 42(22):2360-2367. (in Chinese)

1170 Xue Y.Q., Wu J.C., Ye S.J., Zhang Y.X., 2000. Hydrogeological and hydrogeochemical studies for salt
1171 water intrusion on the South Coast of Laizhou Bay, China. *Ground Water*. 38, 38-45.

1172 Yang H., 1996. Sea-level changes in east China over the past 20000 years. in *Study of Environmental*
1173 *Change*. Hohai University Press. Nanjing, China. pp390-395.

1174 Yang L., 2011. Formation mechanism of bedrock fracture type-geothermal water in Qinhuangdao area.
1175 *West-china Exploration Engineering*. Urumchi, China. 10:151-152. (in Chinese)

1176 Yang Y., Gao S., Xie Y., 2008. Assessment and control countermeasures of seawater intrusion hazard on
1177 Qinhuangdao Region. *The Chinese Journal of Geological Hazard and Control*. 19(3):139-143.
1178 (Chinese with English abstract)

1179 Yang Y., He Q., Xie Y., Cao C., 1994. Grey model prediction of seawater intrusion of Qinhuangdao. *The*
1180 *Chinese Journal of Geological Hazard and Control*. 5(sup.):181-183. (Chinese with English abstract)

1181 Yechieli Y., Kafri U., Sivan O., 2009. The inter-relationship between coastal sub-aquifers and the
1182 Mediterranean Sea, deduced from radioactive isotopes analysis. *Hydrogeology Journal*. 17:265-274.

1183 Zang W., Liu W., Guo J., Zhang X., 2010. Geological hazards of seawater intrusion and its control
1184 measures in Qinhuangdao City, Hebei Province. *The Chinese Journal of Geological Hazard and*
1185 *Control*. 21(4):120-125. (Chinese with English abstract)

1186 Zeng J., 1991. Geochemistry of geothermal water in Qinhuangdao area, Hebei Province. *Bull. Institute of*
1187 *Hydrogeology and Engineering Geology*, Chinese Academy of Geological Sciences. 7:111-127.

1188 Zhang B., 2012. Mechanism of Seawater Intrusion Using Hydrochemistry and Environmental Isotopes in
1189 Qinhuangdao Yang Dai River Plain. Master's Thesis. Xiamen University, Fujian, China. (Chinese with
1190 English abstract)

1191 Zhang Q., Volker R.E., Lockington D.A., 2004. Numerical investigation of seawater intrusion at
1192 Gooburrum, Bundaberg, Queensland, Australia. *Hydrogeol. J.* 12 (6), 674-687.

1193 Zhang Z., Peng L., 1998. Groundwater hydrochemical characteristics on seawater intrusion in eastern and
1194 southern coasts of Laizhou Bay. *China Environmental Science*. 18(2):121-125.

1195 Zhuang Z., Liu D., Yang M., Li H., Qiu H., Ning P., Song W., Xu Z., 1999. The role of anthropogenic
1196 activities in the evolution of saline water intrusion processes. *Journal of Ocean University of Qingdao*.
1197 29(1):141-147. (Chinese with English abstract)

1198 Zuo W., 2006. Survey and Research on Seawater Intrusion in the Yandaihe Plain of Qinhuangdao City.
1199 Doctoral Thesis. China University of Geosciences, Beijing, China. (Chinese with English abstract)

1200 Zuo W., Yang Y., Dong Y., Liang M., 2009. The numerical study for seawater intrusion in Yanghe and
1201 Daihe coastal plain of Qinhuangdao City. *Journal of Natural Resources*. 24(12):2087-2095. (Chinese
1202 with English abstract)

1203